Cretaceous Research 184 (2026) 106355

Contents lists available at ScienceDirect

Cretaceous Research

journal homepage: www.elsevier.com/locate/CretRes

Albian integrated foraminiferal and calcareous nannofossil biostratigraphy in the southern high latitudes (IODP Site U1513, Indian Ocean) across OAE 1d, and correlation to low latitudes

E. Wolfgring [a,*], M.R. Petrizzo [b], D.K. Watkins [c]

[a] Department of Geology, University of Vienna, Josef-Holaubek-Platz 2, A-1090 Vienna, Austria
[b] Dipartimento di Scienze della Terra, Universitá degli Studi di Milano, Milan, Italy
[c] Department of Earth Sciences, University of Nebraska, Lincoln, NE, USA

ARTICLE INFO

Article history:
Received 22 August 2024
Received in revised form
4 February 2026
Accepted in revised form 5 February 2026
Available online 20 February 2026

Keywords:
Albian
Foraminifera
Calcareous nannofossils
Biostratigraphy
OAE
IODP

ABSTRACT

The International Ocean Discovery Program (IODP) drilled Sites U1513, U1514, and U1516 during Expedition 369 that recovered "middle" to Upper Cretaceous sediments in the Mentelle Basin (offshore Australia, Indian Ocean) located at a paleolatitude of 57°S–62°S. While all three sites contain Albian strata, Hole U1513D provides the most extensive and well-preserved record.

Calcareous nannofossils of Site U1513 are relatively diversified and show typical high-latitude assemblages allowing the construction of a biostratigraphic framework. The Albian strata span calcareous nannofossil subzones CC8a to CC9a-b as indicated by the sequential first occurrences of *Tranolithus orionatus*, *Axopodorhabdus biramiculatus*, *Eiffellithus monechiae* and *Eiffellithus turriseiffelii*.

The planktonic foraminiferal biostratigraphy based on the occurrence of *Clavihedbergella simplex*, *Ticinella primula* and *Laeviella bentonensis*, identifies the upper Albian interval, although the lack of marker taxa hampered the application of the tropical-subtropical biozonation. The planktonic foraminiferal assemblage is dominated by the small-sized *Microhedbergella praeplanispira*.

Benthic foraminiferal data document cosmopolitan agglutinated and calcareous taxa and contain the markers *Gavelinella intermedia*, *Osangularia schloenbachi*, as well as taxa typical in high latitudes, e.g., *Eomarssonella crespinae* and *Scutuloris* sp. The lower Albian is dominated by agglutinated foraminifera. Through the middle to lower upper Albian interval, calcareous benthic foraminifera increase in abundance followed by a decline with increasing abundance of agglutinated forms in the upper Albian. In the uppermost part of the studied section a previous publication identifies the Oceanic Anoxic Event 1d by changes in the $\delta^{13}C$ signature. The biostratigraphic data documented in the study at hand support the placement of this event.

1. Introduction

The Albian stage of the Lower Cretaceous in the southern high latitudes has long been the subject of extensive biostratigraphic correlation and interpretation. On a broader scale, documentations of upper Albian microfossil assemblages have predominantly focused on taxonomic descriptions and paleoecological interpretations of assemblages.

Important biostratigraphic results and paleoenvironmental data were published from different regions, including results from deep-sea drilling, such as the South Atlantic and South America (e.g., Malumián, 1982; Krasheninnikov and Basov, 1983; Malumián and Náñez, 2002; Pérez Panera, 2012), the Indian Ocean, particularly focusing on the Kerguelen Plateau and the Western Australian basins, with shorelines extending as far as to the Perth Abyssal Plain or the Naturaliste Plateau (i.e., Haig, 1992; Haig and Lynch, 1993; Huber et al., 1995; Holbourn and Kaminski, 1995; 1997; Haig et al., 1996), India (Venkatachalapathy and Ragothaman, 1995; Das Gupta et al., 2007; Kanungo et al., 2020), and Antarctica (e.g., Leckie, 1990). These discoveries also prompt a closer examination of the Albian paleogeographic configuration within the framework of the breakup of Gondwana, highlighting ongoing divergence of the Australian, Indian and Antarctic plates

* Corresponding author.
E-mail address: erik.wolfgring@univie.ac.at (E. Wolfgring).

https://doi.org/10.1016/j.cretres.2026.106355

and the emergence of new ocean basins during the middle to Late Cretaceous (i.e., Gibbons et al., 2013; Harry et al., 2020; Dummann et al., 2021; Fauth et al., 2023).

The Australian margin displays a unique window into Albian environments, illustrating continental and marine settings. Well constrained by nannofossil biostratigraphy, the microfossils record at Site U1513 register strong terrestrial influence in the lower to middle Albian strata, displaying predominantly agglutinated foraminifera indicative for shallow neritic environments, and is characterized by the absence of planktonic foraminiferal taxa. Subsequently in the middle Albian, this region experienced transitions from shallow epicratonic seas to fully marine conditions, as documented in Ludbrook (1966), Haig (1992), Haig and Lynch (1993), and Campbell and Haig (1999).

During the late Albian, a surge in marine influence was documented in the Mentelle Basin and Naturaliste Plateau, leading to the influx of planktonic foraminifera and the diversification of the calcareous benthic foraminiferal taxa characteristic of deeper depositional environments (middle to outer neritic to upper bathyal). These conditions appear to have ended abruptly and conditions for life in the surface and bottom waters deteriorated as suggested by the rapid decline in planktonic and benthic foraminiferal abundance, correlating with the Oceanic Anoxic Event (OAE) 1d identified by Fan et al. (2022) in Core U1513D based on the diagnostic positive $\delta^{13}C$ signature.

The changes in the foraminiferal assemblages can be correlated with similar results involving black shale deposition during transgressive phases from the Albian sequences in the Southern Hemisphere and particularly at southern high latitudes (Malumián and Ramos, 1984; Holbourn and Kaminski, 1995; Holbourn et al., 2013; Kochhann et al., 2014). The present study aims to establish the biostratigraphic framework of the Albian, draw comparisons with contemporaneous sections, and document changes in benthic environments, underscoring the variability and fragility of high-latitude settings in the Austral Cretaceous record.

2. Study area

International Ocean Discovery Program Sites U1513, U1514 and U1516 are located in the Mentelle Basin on the eastern flank of the Naturaliste Plateau, approximately 400 km offshore southwestern Australia in the south-eastern Indian Ocean (Fig. 1).

The triple junction formed by the Australian, Antarctic, and Indian plates was close to the study region and the Cuvier and Perth Abyssal Plains were affected by the rifting and breakup of East Gondwana that began in the late Valanginian (Wainman et al., 2019, 2020; Huber et al., 2019a; Lee et al., 2020; Harry et al., 2020). The Naturaliste Plateau and Mentelle Basin preserved sediments that were deposited in a thermally subsiding basin after the initial phase of rifting and breakup, that underwent another phase of rifting during the Late Cretaceous (White et al., 2013, 2020).

3. Materials and methods

3.1. Samples

The International Ocean Discovery Program (IODP) Expedition 369 recovered Albian sediments at Sites U1513, U1514 and U1516. The most complete and significant record was retrieved from Site U1513, Hole D, where an approximately 200 m-thick uniform succession of greyish to blackish shaly material characterized by generally low carbonate content was documented (Figs. 2, 3). This study focuses on a ~130 m-thick succession comprising the Albian of Hole U1513D. We correlate the biostratigraphic data to the

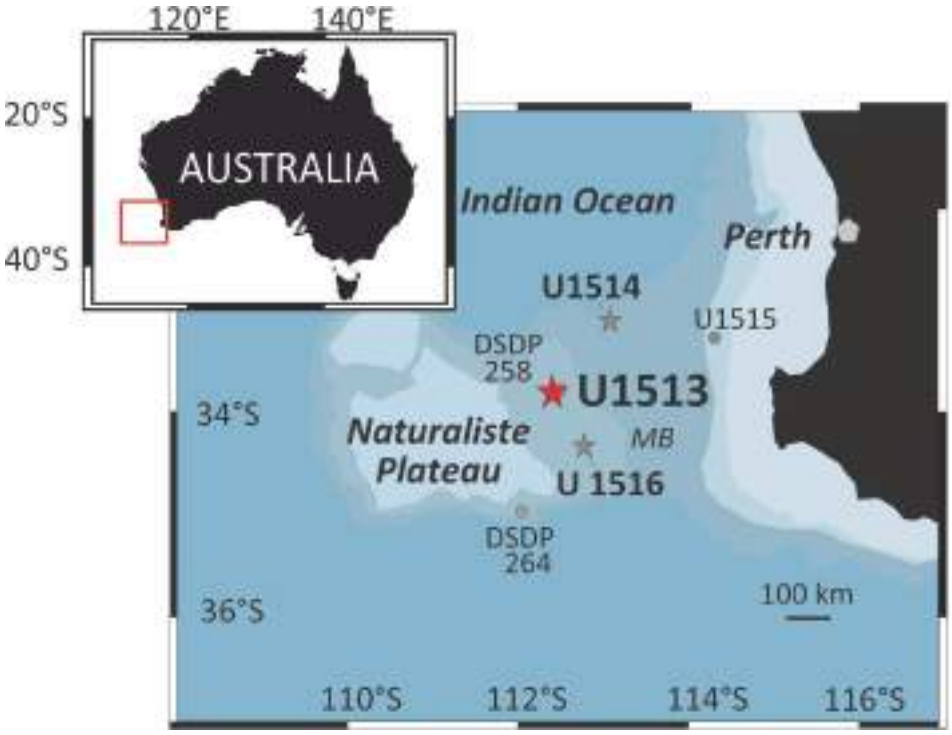

Fig. 1. Map of the studied area in the Mentelle basin (MB) on the eastern flank of the Naturaliste Plateau, offshore western Australia (modified after Wolfgring and Petrizzo, 2024). International Ocean Discovery Program (IODP) Expedition 369 Site U1513 is denoted by a red star, Sites U1514 and 1516 by a gray star. Other sites drilled during IODP Expedition 369 and Deep Sea Drilling Project (DSDP) Site 264 and 258 are denoted by gray circles.

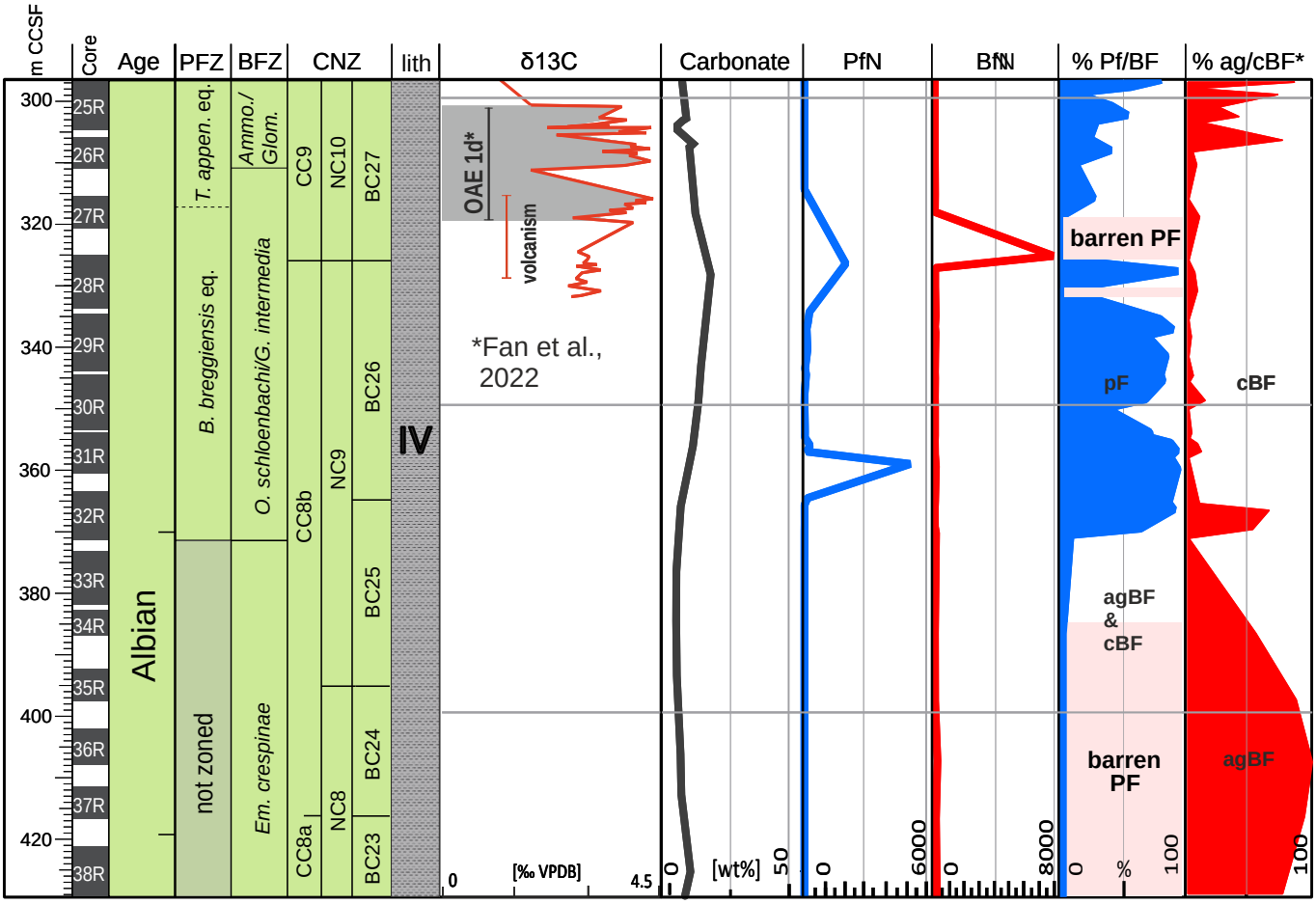

Fig. 2. Core recovery and biostratigraphic framework of the Albian at Site U1513D. Lithology represented by greyish to blackish shales (lithological unit IV) and core recovery after Huber et al. (2019a, 2019b). Calcareous nannofossil and planktonic foraminiferal biozonations and benthic foraminiferal associations recorded at Site U1513D according to this study. Sparse planktonic foraminiferal data and the absence of biostratigraphic markers resulted in the definition of biozones equivalent (eq.) as follows: *B. breggiensis* eq. (=*Biticinella breggiensis* eq.) and *T. appen* eq. (=*Thalmanninella appeninnica* eq.) zones. Relying on only one indicative individual, *B. breggiensis* is shaded grey. *Em. crespinae* = *Eomarssonella crespinae*, *O. schloenbachi* = *Osangularia schloenbachi*, *G. intermedia* = *Gavelinella intermedia*, *Ammo.* = *Ammodiscus*, *Glom.* = *Glomospira*. Carbonate content in [wt%], planktonic and benthic foraminifera per gram of dry sediment, relative abundance of agglutinated and planktonic foraminifera. The position of Oceanic Anoxic Event (OAE) 1d according to Fan et al. (2022) is shaded in grey. Abbreviations: m CCSF = meters Core Composite Depth Below Seafloor; PFZ = planktonic foraminiferal Zone; BFZ = benthic foraminiferal Zone, CNZ = calcareous nannofossil Zone; lith = lithology; Pf = planktonic foraminifera, Bf = benthic foraminifera; PfN = planktonic foraminiferal number, BfN = benthic foraminiferal number, agBF = agglutinated benthic foraminifera; cBF = calcareous benthic foraminifera; * percentage of agBF/cBF relative to total BF.

stratigraphic position of the OAE 1d as defined by Fan et al. (2022), primarily based on the identification of the positive carbonate $\delta^{13}C$ shift coinciding with a negative $\delta^{18}O$ excursion and high total organic carbon (TOC) content between 300 and 320 m CCSF (meters Core Composite Depth below Sea Floor). Data are plotted on the m CCSF depth scale (Huber et al., 2019b).

In this study, we refined the results of IODP Expedition 369 (Huber et al., 2019b) by re-examination of the nannofossil shipboard data and analysis of a new set of samples for foraminiferal investigation.

3.2. Foraminifera and nannofossils

Calcareous nannofossils from 80 samples were examined to elucidate the biostratigraphy of the Albian at Site U1513D from 297.4 to 442.4 m CCSF. The samples were prepared as smear slides of raw sediment and observed at ×1250 magnification. At least 400 fields of view were examined qualitatively per sample to determine species composition, nannofossil preservation state, and total nannofossil relative abundance. The taxonomy of calcareous nannofossils largely follows the Nannotax3 database (https://www.mikrotax.org/Nannotax3/) and biozonation follows the CC zonation of Perch-Nielsen (1985), the NC zonation of Bralower et al. (1995), and the BC zonation of Bown et al. (1998). Nannofossil abundance data are given in the Supplementary Files (St.1) and Fig. 4.

Benthic and planktonic foraminifera were examined from 37 samples. Samples U1513D-25-1, 75–78 cm (297.42 m CCSF) through U1513D-32-5, 52–55 cm (371.40 m CCSF) were weighed, soaked in a solution of H_2O_2 and water, washed over 38, 125 and 250 μm sieves, and dried. If necessary, samples were split to a processable size and subsequently studied for foraminiferal content. The following core catcher samples, prepared shipboard during IODP Expedition 369 were studied: U1513D-32-CC, 21–26 cm (371.40 m CCSF), 1513D-34-CC, 0–5 cm (368.80 m CCSF), U1513D-35-CC, 0–5 cm (379.58 m CCSF), U1513D-36-CC, 0–5 cm (404.37 m CCSF), U1513D-37-CC, 0–5 cm (416.54 m CCSF) and U1513D-38-CC, 0–5 cm (429.08 m CCSF).

Taxonomy of planktonic foraminifera follows Petrizzo et al. (2008, 2012), Petrizzo and Huber (2006), Petrizzo and Gilardoni (2020), and the pforams@mikrotax database at http://www.mikrotax.org/pforams (Huber et al., 2016). Biozonation is

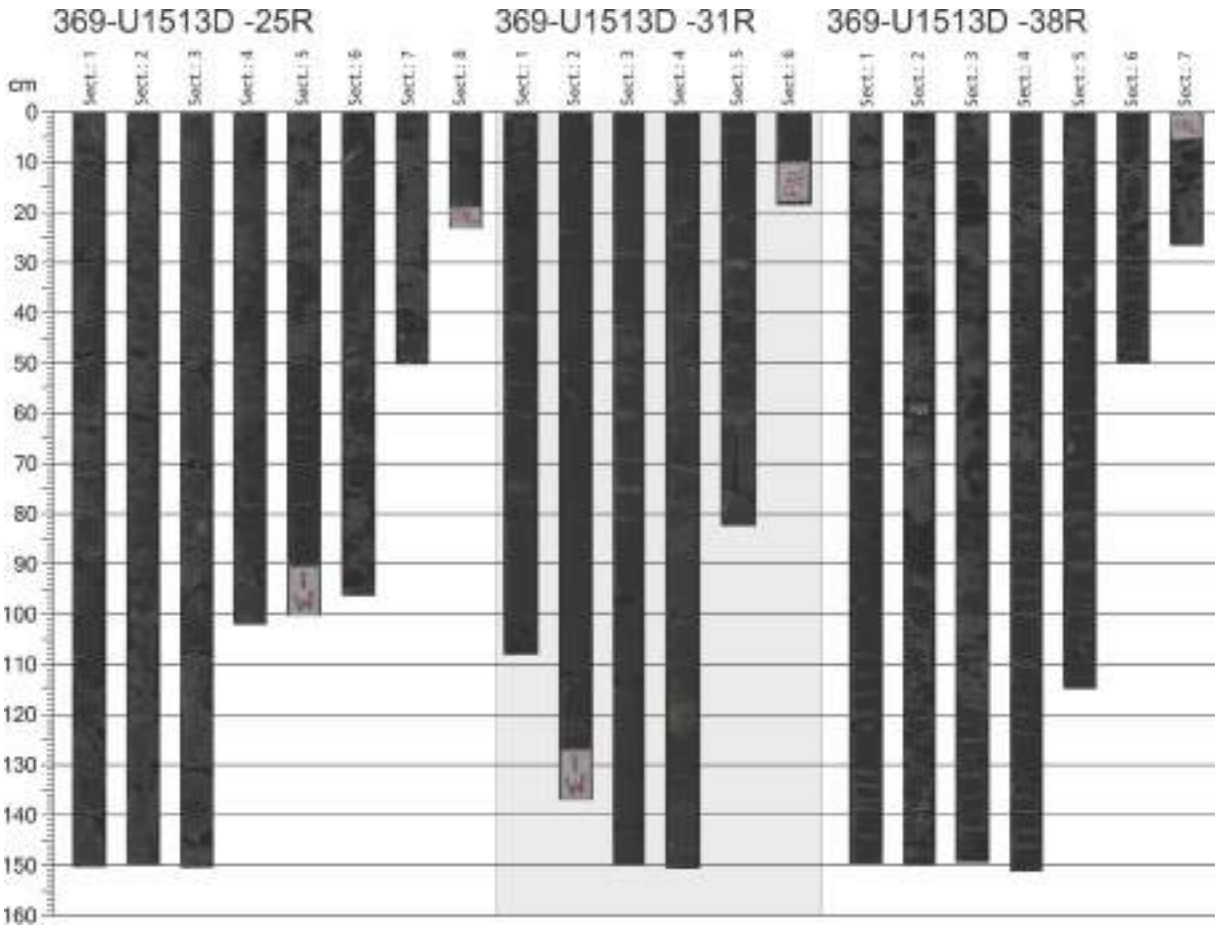

Fig. 3. Core images of Cores U1513D-25R (296.6–306.2 m CCSF), U1513D-31R (354.2–360.66 m CCSF) and U1513D-38R (421.4–429.35 m CCSF) with placeholders for samples taken shipboard for palaeontology and geochemistry, i.e., PAL and IW.

according to Robaszynski and Caron (1995) and Premoli Silva and Sliter (1995), however the absence of biozonal markers resulted in the definition of biozones equivalent interpreted according to the composition of the assemblages.

The taxonomic interpretation of benthic foraminifera predominantly follows Scheibnerová (1976), Holbourn and Kaminski (1995), Tewari et al. (1996), Holbourn and Kaminski (1997), and Holbourn et al. (2001a). As the taxonomic features crucial for the identification of benthic taxa at species level could not be accurately identified in the small size fraction (38–125 μm), this paper entails a genus level identification. Benthic foraminiferal habitat preferences (e.g., oxygenation, infaunal/epifaunal) are interpreted according to Koutsoukos (1989), Koutsoukos and Hart (1990), Kaminski et al. (1995), and Murray et al. (2011). Paleobathymetric classification follows Nyong and Olsson (1984) (<2500 m-abyssal, 1500–2500 m: lower bathyal, 500–1500 m: middle bathyal, 500–200 m: upper bathyal, 200–100 m: outer shelf, 100–50 m: middle shelf, 50–0 m: inner shelf). The terminology relating to oxygen saturation refers to Wignall et al. (2010) (i.e., in descending order of oxygen content: oxic, dysoxic and suboxic).

The assessment of abundance data of benthic and planktonic foraminifera in core catcher samples had to rely on the average weight of the other samples from Site U1513D (the average weight of foraminiferal samples between 297.42 and 369.97 m CCSF is 21.65 g) because core catcher samples were not weighed on board (see Huber et al., 2019a, 2019b). The abundance of benthic and planktonic foraminifera is given in foraminiferal specimens per gram of dry sediment (see Murray and Alve, 2000) as PF/g dry for planktonic foraminifera and BF/g dry for benthic foraminifera. Foraminiferal counts and micrographs of selected species are given in the supplementary files (planktonic foraminifera in St. 2, and benthic foraminifera in St. 3) and in Figs. 4–9.

Selected foraminiferal taxa were photographed using Scanning Electron Microscopy at the Universities of Milan and Vienna (SEM Jeol JSM-IT500 and JEOL JCM-6000, respectively). Nannofossil bioevents and foraminiferal abundance data will be made available in the PANGAEA online repository for Earth and environmental science data (www.pangaea.de). Nannofossil smear slides are deposited at the Earth & Atmospheric Sciences Department at the University of Nebraska-Lincoln, the foraminiferal microslides are stored with the curatorial number “369-U1513D” in the Micropaleontology Collection at the Dipartimento di Scienze della Terra “A. Desio”, Università degli Studi di Milano.

3.3. Position of Oceanic Anoxic Event (OAE) 1d

The placement of OAE 1d in this study is based on the bio- and chemostratigraphic framework established in Fan et al. (2022), who identified the event by following the multiple positive carbon isotope peaks diagnostic for OAE1d within the interval between 319 m and 299 m CCSF (Fig. 2). We used the geochemical data presented in the aforementioned publication as stratigraphic markers and observed and correlated biostratigraphic and paleoecological observations to this interval.

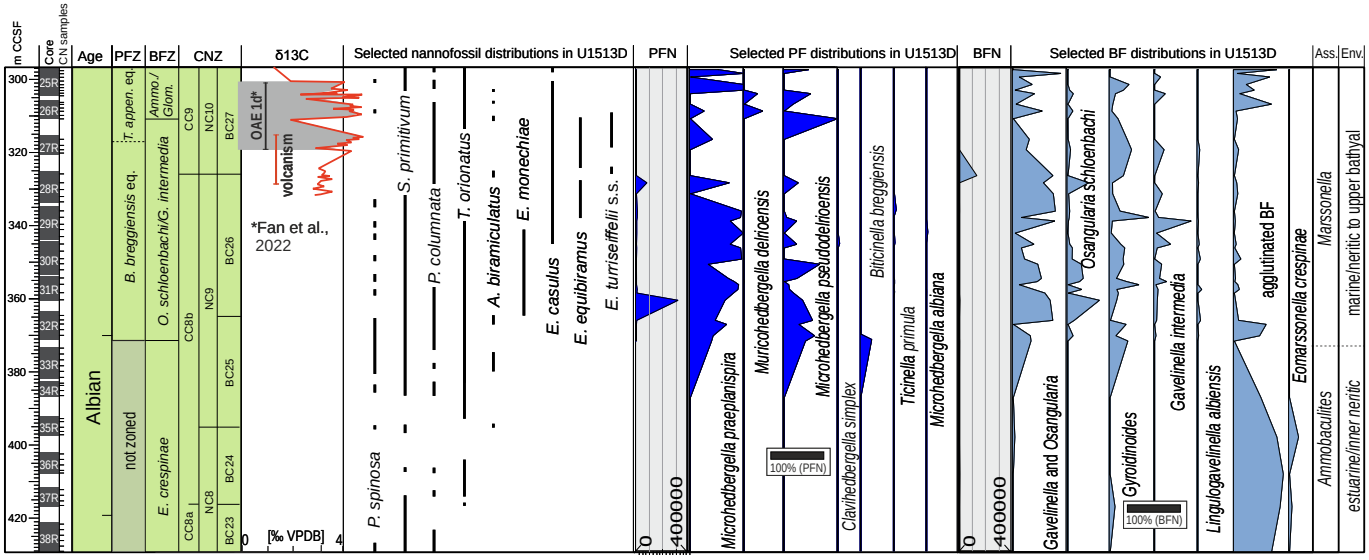

Fig. 4. Core recovery and nannofossil sample positions, Albian calcareous nannofossil, planktonic and benthic foraminiferal biostratigraphy of Hole U1513D. The planktonic foraminiferal zone (PFZ) and benthic foraminiferal zone (BFZ) are indicated as well as three calcareous nannofossil zonations (CNZ): the CC zonation of Perch-Nielsen (1985), the NC zonation of Bralower et al. (1995), and the BC zonation of Bown et al. (1998). Total abundance of planktonic (blue) and benthic (light blue) foraminifera and selected biostratigraphically and palaeoecologically noteworthy taxa in percent of the total abundance of the respective group are shown. The position of OAE 1d according to Fan et al. (2022) is shaded in grey. Abbreviations: m CCSF = meters Core Composite Depth Below Seafloor; PFZ = planktonic foraminiferal Zone; BFZ = benthic foraminiferal Zone; PFN = planktonic foraminiferal number; BFN = benthic foraminiferal number; PF = planktonic foraminifera, BF = benthic foraminifera; PFN = planktonic foraminiferal number; BFN = benthic foraminiferal number; Ass. = benthic foraminiferal association (after Haig, 1992); *B. breggiensis* eq. = *Biticinella breggiensis* equivalent, and *T. appen* eq. = *Thalmanninella appenninica* equivalent zones. *E. crespinae* = *Eomarssonella crespinae*; *O. schloenbachi* = *Osangularia schloenbachi*; *G. intermedia* = *Gavelinella intermedia*; *Ammo.* = *Ammodiscus*; *Glom.* = *Glomospira*; *P. spinosa* (=*Prediscosphaera spinosa*); *S. primitivum* (=*Staurolithites primitivum.*); *P. columnata* (=*Prediscosphaera columnata*); *T. orionatus* (=*Tranolithus* orionatus); *A. biramiculatus* (=*Axopodorhabdus biramiculatus*); *E. monechiae* (=*Eiffellithus monechiae*); *E. casulus* (=*Eifellithus casulus.*); *E. equibiramus* (=*Eiffellithus equibiramus*); *E. turriseiffelii* s.s. (=*Eiffellithus turriseiffelii* sensu stricto).

4. Results

4.1. Calcareous nannofossils

Calcareous nannofossil assemblages at the base of the Albian section (421.7–435.8 m CCSF) include *Prediscospahera spinosa*, *P. columnata*, *Seribiscutum primitivum*, and *Hayesites albiensis* but lack *Tranolithus orionatus*. This association indicates the lower Albian Zone BC 23 (=Subzone CC8a). Nannofossils are sparse and poorly preserved at the base of this interval (below 430 m CCSF) but are common and well-preserved in the upper portion of Zone BC23 (Fig. 4). The interval from the First Appearance Datum (FAD) of *Tranolithus orionatus* at 416.5 m CCSF to the FAD of *Axopodorhabdus biramiculatus* (=*A. albianus* of some authors) at 395.1 m CCSF contains generally poorly preserved, sparse assemblages typical of Zone BC24. These poorly preserved, sparse calcareous nannofossil assemblages continue through the lower 10 m of the overlying Zone BC25, which includes the interval from the FAD *A. biramiculatus* to the FAD of *Eiffellithus monechiae* at 364.6 m CCSF (Fig. 4). Nannofossil abundance is much higher in Zones BC25 and BC26 than in the underlying zones at Site 1513. The best preservation at Site 1513 is observed in Zone BC26 which spans the interval from the FAD of *E. monechiae* to the FAD of *Eiffellithus turriseiffelii* (s.s.) at 325.8 m CCSF (Fig. 4, St.1). The FAD of *E. turriseiffelii* marks the base of CC9, NC10, and BC27. As used herein, this marks the first appearance of the large forms (>8 μm) that are typical of the species. Smaller, morphologically similar species such as *E. casulus* and *E. equibiramus*, occur in the underlying BC26 assemblages. Nannofossil abundance and preservation degrade upwards in this zone at Site U1513, so that the upper few meters contain only rare, poorly-preserved nannofossils that are difficult to precisely date.

4.2. Planktonic foraminifera

The abundance of planktonic foraminifera varies through the Albian, while they are absent in the lowermost part of section (429.08–386.8 m CCSF) (Figs. 4 and 5, St. 2), the numbers of planktonic foraminifera fluctuate between 8 and 109 PF/g dry sediment in samples 371.4, 369.97, and 366.87 m CCSF (Fig. 5). Overall, 14 species in two planktonic foraminiferal zones were documented. Fig. 6 illustrates selected planktonic foraminiferal taxa.

The planktonic marker *Biticinella breggiensis* occurs in sample U1513D 32R-CC 21–26 cm (at 371.40 m CCSF) above the lowermost interval of the Hole 1513D virtually barren of calcareous foraminifera. We document an increase in the abundance of planktonic foraminifera from 365.77 m CCSF upsection, recording 148 PF/g dry sediment in 356.77 m CCSF, followed by the highest abundance with 5237 PF/g and a subsequent gradual decline to only 5 PF/g dry sediment in sample 350.47 m CCSF. Above this sample, planktonic foraminiferal numbers show another gradual increase with an average of 103 PF/g (between 5 and 250 PF/g) at 350.47 and 335.99 m CCSF. Above a barren interval at 331.26 m, another local maximum of 2044 PF/g is reached, followed by another barren interval between 326.32 and 319.24 m CCSF. Coinciding with the position of OAE 1d as identified by Fan et al. (2022), planktonic foraminiferal abundance declines from 277 PF/g to 1.7 PF/g between 316.41 and 297.42 m CCSF (Figs. 4 and 5). Foraminiferal biostratigraphic data do not show tropical-subtropical marker taxa and rely on the documentation of *Clavihedbergella simplex* (from 358.33 through 337.72 m CCSF), *Ticinella primula* (from 358.33 through 328.27 m CCSF), and *Laeviella bentonensis* (from 354.33 through 306.83 m CCSF), which allow the identification of the upper Albian stratigraphic interval. The planktonic foraminiferal assemblage

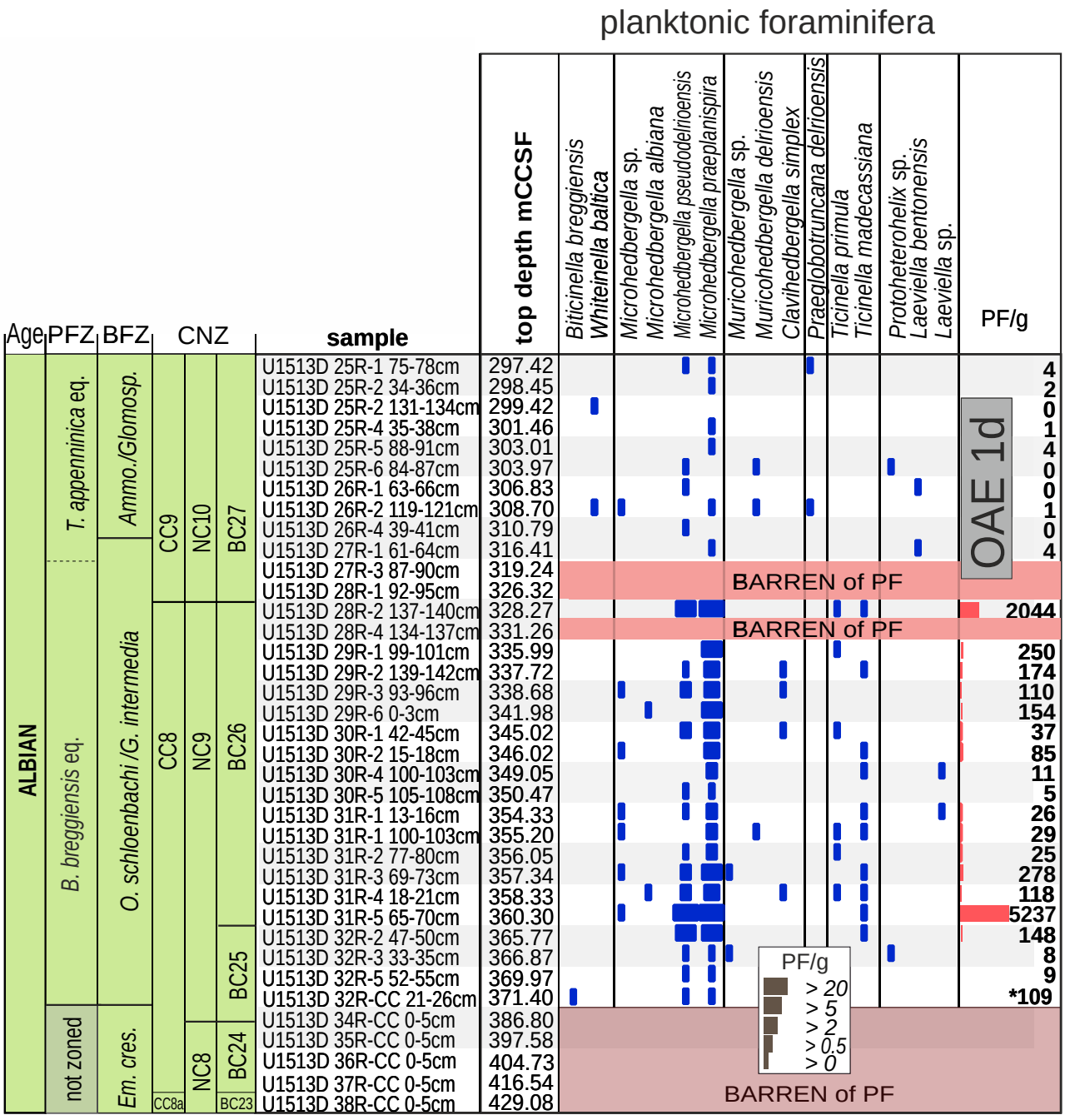

Fig. 5. Biostratigraphic framework of Site U1513. Abundance of planktonic foraminifera per gram of dry sediment (PF/g). OAE 1d (Fan et al., 2022) shaded in grey, levels barren of planktonic foraminifera (PF) are shaded in red. PF/g marked with an * refer to the average weight of CC samples (see Section 3.2). Abbreviations: m CCSF = meters Core Composite Depth Below Seafloor; PFZ = planktonic foraminiferal Zone; BFZ = benthic foraminiferal Zone; CNZ = calcareous nannofossil Zone.

documented between 371.40 and 297.42 m CCSF at Site U1513 is dominated by the small-sized *Microhedbergella praeplanispira* in association with a considerable presence of *Microhedbergella pseudodelrioensis* (Figs. 4 and 5, and Supplementary Material St. 2).

The sole occurrence of *Biticinella breggiensis* was recorded in sample U1513D 32R-CC 21–26 cm at 371.4 m CCSF and allow identification of the *Biticinella breggiensis* eq. Zone, which characterizes planktonic foraminiferal assemblages between 371.4 and 316.41 m CCSF. The *Thalmanninella appenninica* equivalent Zone is identified above the barren interval in Core 27R. The base of the *T. appenninica* equivalent Zone is marked by the concomitant presence of *Praeglobotruncana delrioensis* and *Laeviella bentonensis* that are reported to have their LOs in the *T. appenninica* Zone (Petrizzo et al., 2008), providing a robust biostratigraphic marker even in the absence of the nominal index taxon and often correlate with the onset of OAE 1d (Petrizzo et al., 2008).

4.3. Benthic foraminifera

This study assesses 37 samples for benthic foraminiferal stratigraphy and paleoenvironmental implications and recorded 100 benthic foraminiferal taxa (Figs. 4 and 7). Benthic foraminifera show a moderate preservation throughout. Variations in the abundance of benthic foraminiferal taxa at Site U1513 correlate

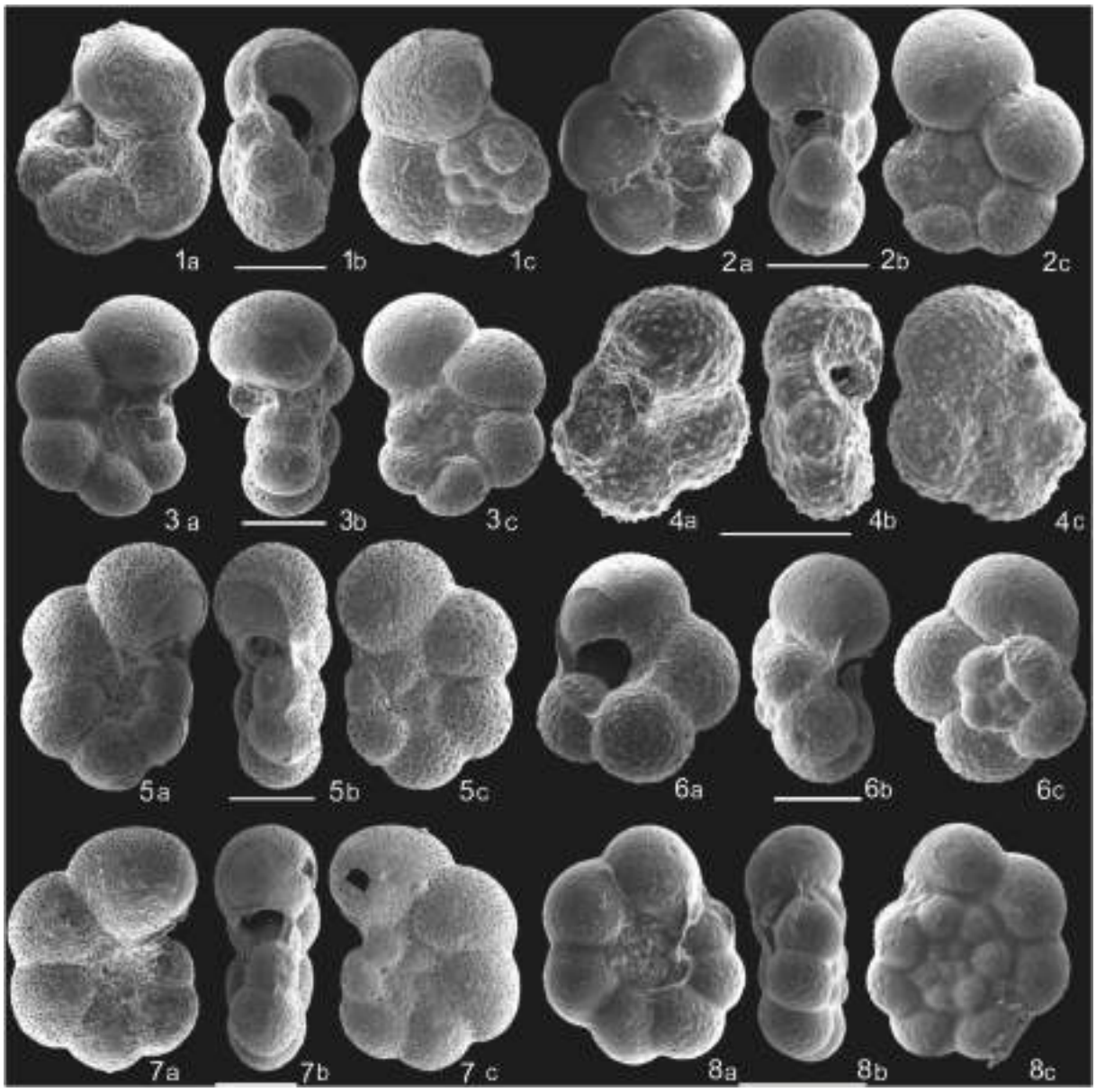

Fig. 6. Planktonic foraminifera of the Albian of Hole U1513D (specimens deposited under the curatorial number "369-U1513D" in the Micropaleontology Collection at the Dipartimento di Scienze della Terra "A. Desio", Università degli Studi di Milano: 1a–c, *Microhedbergella albiana* (Boudagher-Fadel et al., 1996), 369-U1513D-29R-6, 0–3 cm; 2a–c, *Ticinella madecassiana* Sigal 1966, 369-U1513D-29R-2, 139–142 cm; 3a–c, *Ticinella madecassiana* Sigal 1966, 369-U1513D-31R-1, 13–16 cm; 4a–c, *Muricohedbergella delrioensis* (Carsey 1926), 369-U1513D-31R-1, 100–103 cm; 5a–c, *Ticinella primula* Luterbacher 1963, 369-U1513D-31R-3, 69–73 cm; 6a–c, *Microhedbergella pseudodelrioensis* Huber and Leckie, 2011, 369-U1513D-31R-4, 18–21 cm; 7a–c, *Ticinella primula* Luterbacher 1963, 369-U1513D-31R-5, 67–70 cm; 8a–c, *Microhedbergella praeplanispira* Huber and Leckie 2011, 369-U1513D-29R-2, 139–142 cm. Scale bar = 100 μm, a: umbilical, b = lateral, c = spiral view.

with greater changes observed in planktonic foraminifera (Figs. 4 and 7, Supplementary Material St. 3). Figs. 8 and 9 illustrate selected benthic foraminiferal taxa.

The interval 429.08–386.80 m CCSF (Figs. 4 and 7) is barren of planktonic foraminifera and the benthic foraminiferal assemblage is predominantly composed of agglutinated taxa (Figs. 2, 4, and 7). The interval yields a benthic foraminiferal association characterized by the high abundance of the species *Kalamopsis grzybowskii*, *Trochammina minuta* and the occurrence of *Eomarssonella crespinae* hence, the interval is tentatively assigned to the *Eomarssonella crespinae* Zone of Haig, 1979; Haig and Lynch, 1993. The abundance of benthic foraminifera is based on the average weight of samples (see Section 4), resulting in an average of 71.5 benthic foraminifera (BF) per gram of dry sediment (Fig. 7): The four lowermost samples (U1513D 38R-CC – 35CC, 429.08 m – 397.58 m CCSF) are dominated by species like *Kalamopsis grzybowskii*, *Ammodiscus cretaceus*, *Glomospira charoides* or *G. gracilima*. These samples also exhibit a high occurrence of *Recurvoides* and *Haplophragmoides* spp., as well as *Trochammina minuta*, in association with *Textulariopsis elegans* and *Spiroplectammina* sp. Most of these species show a density exceeding 2 BF/g of dry sediment. Calcareous benthic foraminifera are comparatively rare and represented by the cosmopolitan taxa *Dentalina communis*, *Saracenaria* sp., *Praebulimina* sp. and *Gyroidinoides* sp. that are all present in more than 5 BF/gram dry sediment. *Gavelinella* sp. is recorded in one sample at 386.80 m CCSF with 0.41 BF/gram dry sediment (Fig. 7).

Between 371.40 and 310.79 m CCSF, calcareous benthic foraminifera increase in abundance (see Figs. 2, 4, 7). The most

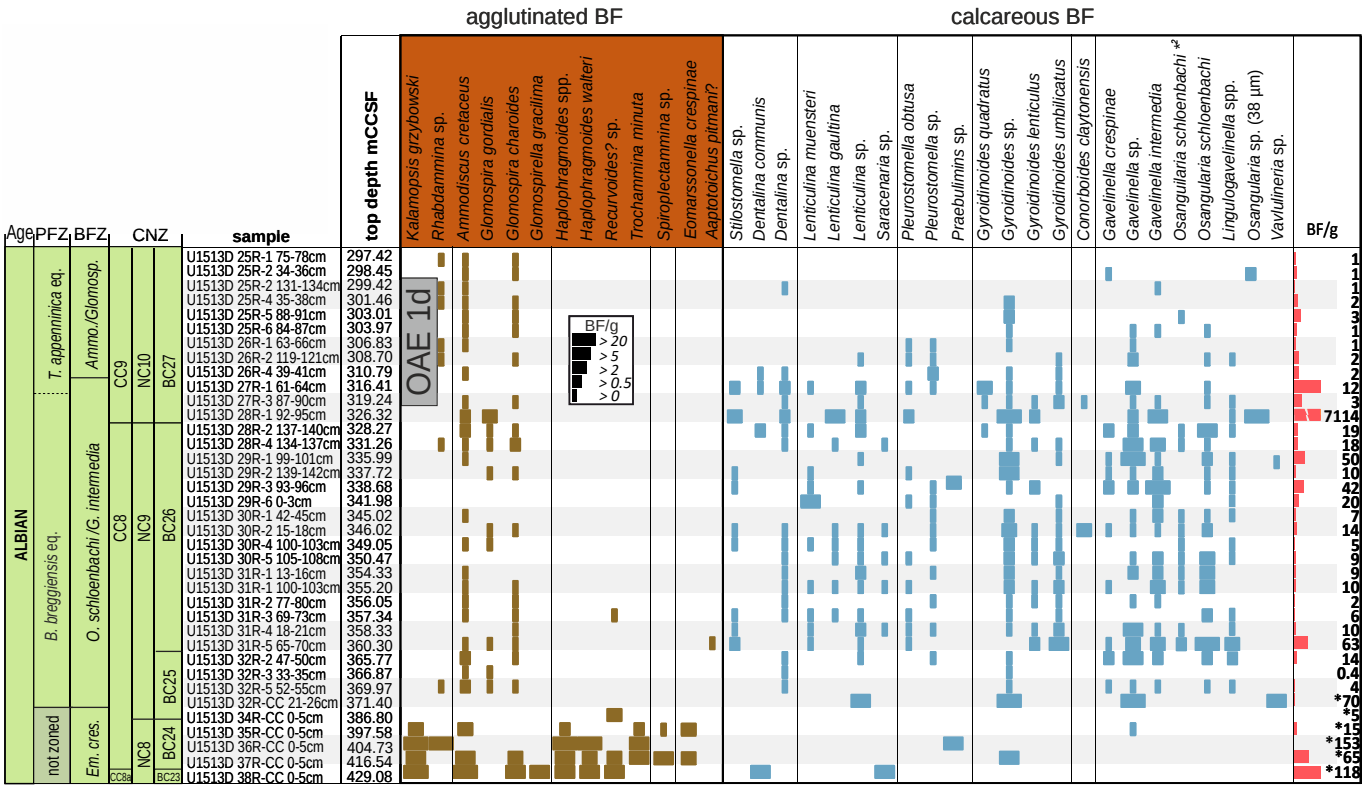

Fig. 7. Biostratigraphic framework of Site U1513. Abundance of benthic foraminiferal taxa with more than 0.5% of the total assemblage or biostratitgraphic or paleoecologic significance per gram of dry sediment (BF/g). BF/g marked with an * refer to the average weight of CC samples (see Section 3.2), note that total BF/g are not to scale in sample 28R1 92–95 m. OAE 1d (Fan et al., 2022) shaded in grey. *2 *Osangularia schloenbachi* type 2 of Holbourn et al. (2001a). Abbreviations: mCCSF = meters Core Composite Depth Below Seafloor; PFZ = planktonic foraminiferal Zone; BFZ = benthic foraminiferal Zone; CNZ = calcareous nannofossil Zone.

frequently documented benthic foraminifera are *Osangularia* (*Gavelinella*) *schloenbachi* and *Gavelinella intermedia*. In average, this section yields 297.91 BF/g dry sediment. This high average abundance can be attributed to the extraordinary high number of benthic foraminifera (7113.95 BF/g dry sediment) recovered in sample U1513-28R-1, 92–95 cm (326.32 m CCSF). Apart from this sample, this interval displays an average of 15.03 BF/g dry sediment and is characterized by the presence of a well-diversified benthic foraminiferal assemblage dominated by calcareous taxa (Fig. 7). The lowermost sample in this interval at 371.40 m CCSF is barren of agglutinated foraminifera and yields *Gyroidinoides* sp. and *Lenticulina* sp. (23 BF/g dry sediment each), *Valvulineria* sp. and *Gavelinella* sp. (11 BF/g dry sediment each). Apart from samples U1513D-32R-5, 52–55 cm and U1513D-32R-2, 47–49 cm (at 369.97 and 366.87 m, documenting 50% and 60% of agglutinated foraminifera, respectively) the percentage of agglutinated foraminifera reaches the 4.4% and rarely exceeds 10% in some isolated samples. *Stilostomella* and *Dentalina* spp. show a patchy presence between 371.4 and 310.79 m, and members of *Lenticulina* and *Gyroidinoides* are almost consistently present apart from 371.4 to 365.77 m CCSF. We document *Lenticulina* sp., *L. muensteri*, *L. gaultina* or *Gyroidinoides* sp., *G. lenticulus*, *G. umbilicatus* and sparsely *G. quadratus*, the latter presenting the highest number in BF/g recorded in the Albian, coinciding with the onset of the OAE 1d (Figs. 4 and 7, Supplementary Table St. 2). *Gyroidinoides*, gavelinellids and *Osangularia* dominate the assemblage in this interval. Apart from the Austral taxa *Gavelinella crespinae* and *Lingulogavelinella indica*, the marker taxa for the middle Cretaceous *Gavelinella intermedia* and *Osangularia schloenbachi* are most frequently recorded in this interval (234 BF/g in average showing abundance maxima at 362 and 328 m CCSF, respectively). *Conorboides claytonensis*, a species that was documented from the middle Cretaceous of Queensland and the Great Artesian Basin in Australia (Ludbrook, 1966; Haig 1979), the Falkland Plateau (DSDP Site 327, Scheiberová, 1981) and the western Australian margin during and after the Oceanic Anoxic Event 2 (Petrizzo et al., 2022; Wolfgring et al., 2023; Wolfgring and Petrizzo, 2024), has been recorded in two samples at Hole U1513D (U1513D-23R-3, 87–90 cm and U1513D-30R-2, 15–18 cm), suggesting a broad distribution of this taxon in the Southern High Latitudes. The taxonomic composition of this interval registers elements with outer neritic to bathyal ranges, i.e., *Osangularia schloenbachi* and other osangularids, *Gavelinella intermedia*, *Lingulogavelinella* sp., *Gyroidinoides* spp.

Overlying the highest occurrence of benthic foraminifera at 326.32 m (in sample U1513D-28R-1, 92–95 cm) and correlating to the position of OAE 1d (spanning U1513D-27R-3, 87–90 cm through U1513D-25R-2, 131–133 cm, 319.24–299.42 m CCSF), the abundance of this group starts to diminish dramatically from core U1513D-26R (310.79 m) onwards and never again reaches values as high as in the interval below (see Figs. 4, 7).

From 310.79 through 297.42 m CCSF, representing the top of the section, a shift from mainly calcareous benthic- to agglutinated benthic foraminifera is observed. Coinciding with a drop in the abundance of benthic foraminifera from 15.03 BF/g to 1.49 BF/g dry sediment. A shift in dominant calcareous

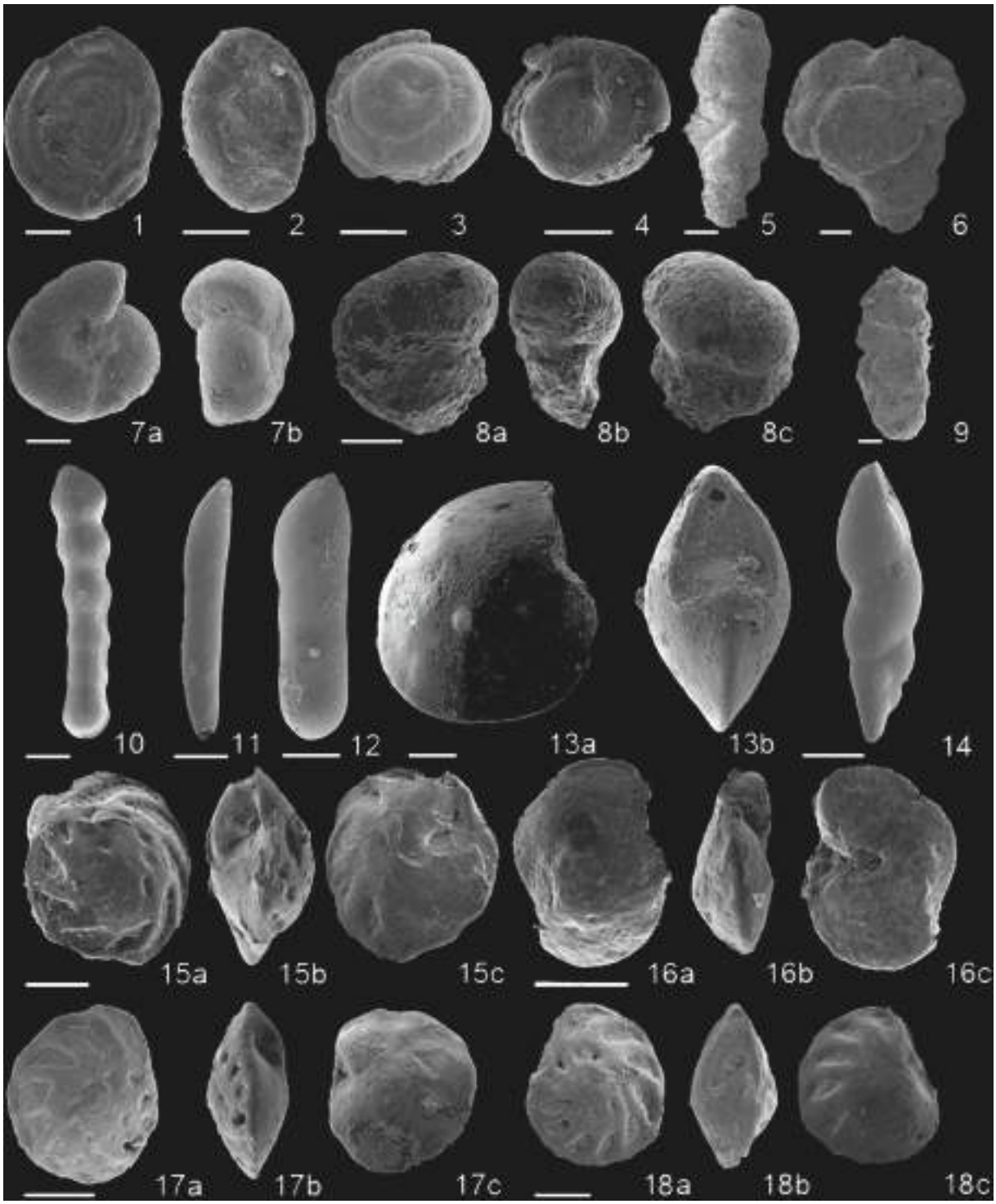

Fig. 8. Benthic foraminifera of the Albian of Hole U1513D (specimens deposited under curatorial number "369-U1513D" in the Micropaleontology Collection at the Dipartimento di Scienze della Terra "A. Desio", Università degli Studi di Milano (1/2): 1. *Ammodiscus cretaceus* (Reuss, 1845), U1513D 31R-5, 65–70 cm; 2. *Ammodiscus peruvianus* Berry, 1928, U1513D 31R-5, 65–70 cm; 3. *Glomospira charoides* (Jones and Parker, 1860), U1513D 31R-5, 65–70 cm; 4. *Glomospira charoides* (Jones and Parker, 1860), U1513D 31R-5, 65–70 cm; 5. *Aaptotoichus* sp., U1513D 31R-5, 65–70 cm; 6. *Eomarssonella crespinae* (Ludbrook, 1966), U1513D, 35RCC; 7a–c. *Haplophragmoides* sp. (?), U1513D, U1513D, 35RCC; 8a–c. *Trochammina minuta* Crespin, 1953, U1513D 35RCC; 9. *Gaudryina* sp., U1513D 35RCC, 0–5 cm; 10. *Dentalina communis* (d'Orbigny, 1825), U1513D 28R-2, 137–140 cm; 11. *Laevidentalina gracilis* (d'Orbigny, 1840), U1513D 28R-2, 127–140 cm; 12. *Astacolus* cf. *compressus* (Cushman, 1917), U1513D-35RCC, 0–5 cm; 13a,b. *Lenticulina muensteri* (Roemer, 1839), U1513D 28R-2, 137–140 cm; 14. *Pleurostomella subnodosa* (Reuss, 1851), U1513D-30-2, 15–18 cm; 15a–c. *Osangularia schloenbachi* (Reuss, 1863), U1513D-28-2, 137–140 cm; 17, 18a–c. *O. schloenbachi* (Reuss, 1863), U1513D 31R-5, 65–70 cm (type 1 of Holbourn et al., 2001a)); 16a–c) *O. schloenbachi* (Reuss, 1863) (type 2 of Holbourn et al., 2001a), U1513D-28-2, 137–140 cm. Scale bar = 100 μm, a: spiral, b = lateral, c = umbilical view.

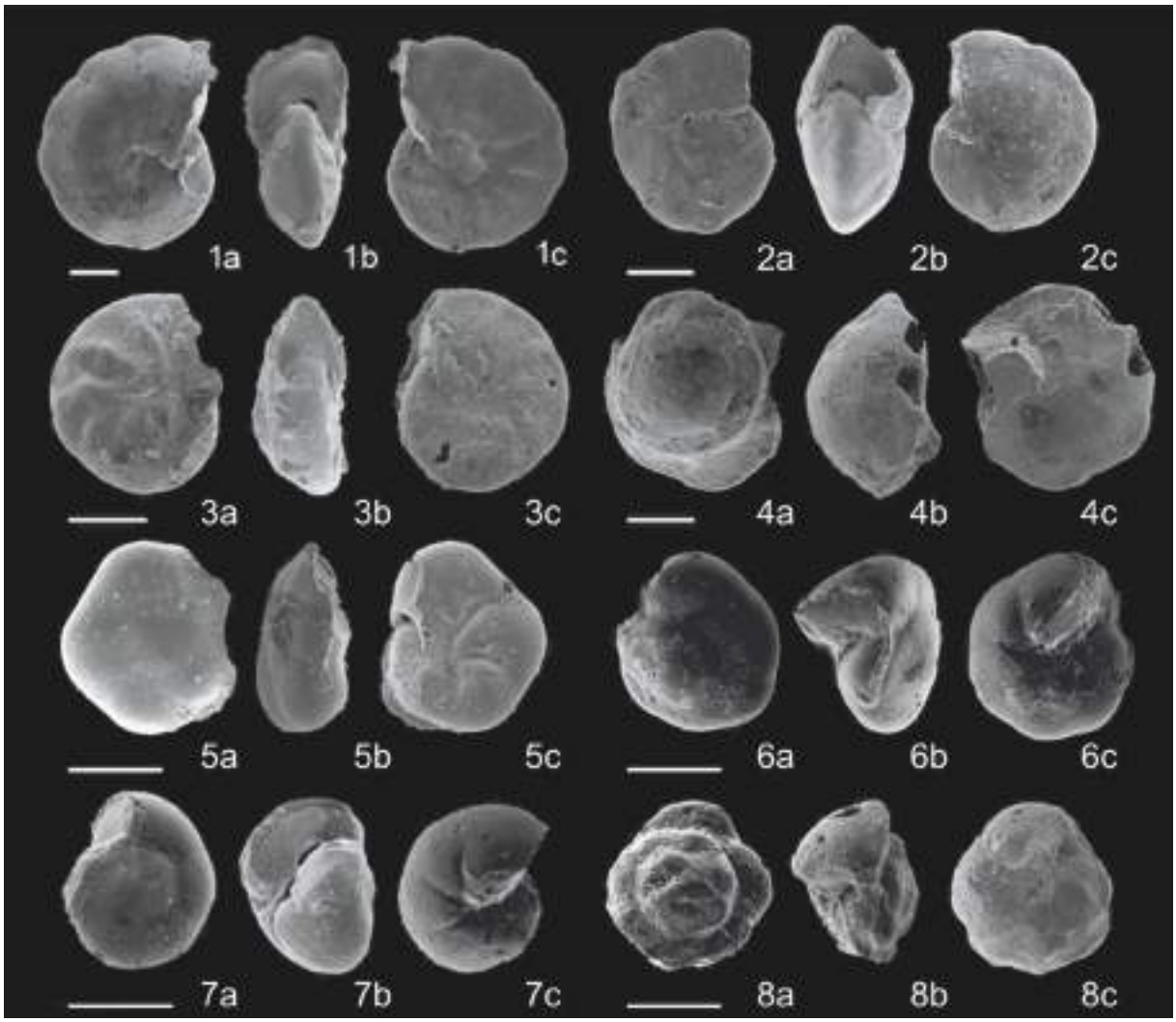

Fig. 9. Benthic foraminifera of the Albian of Hole U1513D (specimens deposited under curatorial number "369-U1513D" in the Micropaleontology Collection at the Dipartimento di Scienze della Terra "A. Desio", Università degli Studi di Milano) (2/2): 1, 2a–c. *Gavelinella intermedia* (Berthelin, 1880), U1513D 28R-1, 92–95 cm; U1513D-31RCC; 3a–c. *Gavelinella* sp. (*G.* cf. *barremiana*? Bettenstaedt), 1952, U1513D 28R-1, 92–95 cm; 4a–c. *Conorboides claytonensis* Ludbrook, 1966, U1513D-30-2, 15–18 cm; 5a–c. *Lingulogavelinella* cf. *indica* Scheibnerová, U1513D-28-2, 137–140 cm; 6a–c. *Gyroidinoides lenticulus*? (Reuss, 1845), U1513D 28R-2, 137–140 cm; 7a–c. *Gyroidinoides umbilicatus* (d'Orbigny, 1840), U1513D 30R-2, 15–18 cm; 8a–c. *Gyroidinoides quadratus* (Cushman and Church, 1929), U1513D 28R-2, 137–140 cm. Scalebar = 100 μm, a: spiral, b = lateral, c = umbilical view.

benthic foraminifera in favour of *Ammodiscus* and *Glomospira* is recorded. The nodosariids, *Lenticulina* and most *Gyroidinoides* virtually disappear. Calcareous taxa are illustrating a patchy distribution of e.g., *Osangularia* (*Osangularia* sp., and *O. schloenbachi*) and *Gavelinella* (*Gavelinella* sp., *G. intermedia* and *G. crespinae*). Calcareous benthic and agglutinated taxa never show a higher density than 0.5 BF/g dry sediment (see Figs. 2, 4, 7).

Benthic foraminiferal assemblages show a clear alternation in dominance between the *Ammobaculites* and *Marssonella* associations of Haig (1979) and Haig and Lynch (1993), with neither being exclusive. At Hole U1513D, dominant agglutinated taxa, including species such as *Eomarssonella* (*Riyadhella*) *crespinae*, *Lingulogavelinella albiensis*, *Trochammina* sp. and *Aaptotoichus pitmani*, accompanied by only few calcareous taxa were assigned the shallow-water *Ammobaculites* association that dominates from the base of the section to 371.40 m CCSF. In contrast, the probably deeper mid-neritic to upper bathyal fully marine benthic foraminiferal fauna dominated by calcareous forms, species like *Gavelinella berthelini*, *Gavelinella intermedia*, *Pleurostomella* sp., *Ammodiscus* sp., and associated planktonic taxa, can be assigned to the *Marssonella* association. The *Marssonella* association is dominant through the remainder of the Albian (Fig. 4).

5. Discussion

5.1. Correlations from high to low latitudes

We compare stratigraphic data from Site U1513 to sections from the Austral realm (e.g., Scheibnerová, 1974, 1976; Haig, 1979, 1992), as well as to other Albian sections globally. Planktonic and benthic foraminiferal biostratigraphy, alongside calcareous nannofossil zonations and, if available, carbon isotope stratigraphy provides a framework for correlating events. Correlations with well-documented sections, such as the Blake Nose Plateau (North Atlantic) (Wilson and Norris, 2001; Petrizzo et al., 2008), Umbria-Marche Basin (Western Tethys) (Giraldo-Gómez et al., 2023), and Shatsky Rise (Central Pacific) (Giraldo-Gómez et al., 2022), allow for a more comprehensive assessment of biostratigraphic patterns and carbon isotope excursions (Fig. 10).

5.1.1. Austral realm and eastern Indian Ocean records

The micropaleontological data collected at Site U1513D can be correlated to the Australian and the eastern Indian Ocean records (Fig. 10). Two other deep sea drilling sites document the Albian in the Austral realm, DSDP Site 259 (Fig. 10.2a) and ODP Site 766 (Fig. 10.2b) (e.g., Ludbrook, 1966; Scheibnerová, 1974; Scheibnerová, 1976; Haig, 1979, 1992; Haig and Lynch, 1993; Haig et al., 1996) (Fig. 10). For these sites the correlation with planktonic foraminifera mostly relies on the presence of *Muricohedbergella* (=*Hedbergella*) *planispira*, with no occurrences of *Ticinella* or *Biticinella* as mentioned in Haig (1992) and Haig and Lynch (1993).

Planktonic foraminiferal information from Site 259 finds, according to Krasheninnikov and Basov (1983), a continuous presence of *Hedbergella infracretacea*, and *Muricohedbergella.* aff. *delrioensis*, thus, assigning it an Albian age (Fig. 10). However, as these two species do not overlap in their stratigraphic ranges (*H. infracretacea* is an Aptian species, *Muricohedbergella delrioensis* an Albian species), we suppose the taxon *H. infracretacea* was misidentified in Krasheninnikov and Basov (1983).

According to Haig (1992), the succession documented from ODP Site 766 in the Cuvier Abyssal Plain, can be interpreted to mark the Aptian-Albian transition (Fig. 10 nr.2b). In the study of Haig (1992), the stratigraphically lower samples from Site 766 (samples 766-25RCC, 230 m to 766-21R-1, 90–94 cm, 192 m) were assigned to the Aptian. Planktonic foraminiferal data published by Haig (1992) from Site 766, were interpreted to display an Aptian age based on the presence of *Globigerinelloides aptiense*, and *Blefuscuiana* (=*Hedbergella*) *aptica* (a junior synonym of *Hedbergella infracretacea*) (see Fig.10.2a).

However, the assemblage, documented at Site 766 (below sample 766-25R-1, 33–35 cm), that indicates an Aptian age is overlain by the lowest occurrence of *Muricohedbergella planispira* already in sample 25R-1, 33–35 (230 m). This suggests that sample 25RCC (add meters) marks the Aptian/Albian boundary, indicating that all sediments above 25RCC are of Albian age, while all sediments below it are of Aptian age (Huber and Leckie, 2011; Petrizzo et al., 2012).

Similarities in Albian benthic foraminiferal stratigraphy of the two Australian deep-sea drill sites, are documented by the presence of key markers correlating with Site U1513D that include *Gavelinella intermedia* and *Osangularia schloenbachi* (referred to as *Osangularia utaturensis* in Scheibnerová, 1974) (Fig. 10.2a, 10.2b), as well as *Lingulogavelinella indica* at Site 259 (as *Orithostella indica* in Scheibnerová, 1974) (Fig. 10.2b).

During the middle to late Albian, benthic foraminiferal assemblages in New South Wales, the Great Artesian Basin, and Eromanga Basin, Queensland, and northeastern Australian and Papuan localities (Laura Basin, Ok Kam region) illustrate a transgression from a shallow epicontinental to an outer neritic and upper bathyal environment (Haig and Lynch, 1993, for the northeastern Australian and Papuan successions; Scheibnerová, 1976; Ludbrook, 1966, for the Great Australian Basin and Queensland, Australia).

Exemplified in sections studied from the Eromanga Basin in Haig and Lynch (1993) (the stratigraphy of the industry well "Hughenden 7" is illustrated in Fig. 10), Albian strata are marked by the *Eomarssonella crespinae* Zone, which defines the early Albian and is correlated with coeval Albian strata in other regions (Haig, 1979; Campbell and Haig, 1999). Above this, the assemblages indicate the transition to the late early Albian to middle Albian, marking the first widespread planktonic incursion into the Eromanga Basin illustrating a transgressive episode. In this context, benthic foraminiferal data illustrate the transition from the *Ammobaculites* to the *Marssonella* benthic foraminiferal association, first described from the Cretaceous of Queensland, Australia by Haig (1979). A similar succession of benthic foraminiferal associations is evident at Site U1513D (see Section 3.1,Figs. 4, 10.1, 10.2b).

Another classic study of Haig et al. (1996; 2004) documents a similar setting for the Gearle Siltstone. This section exhibits a stratigraphic setting comparable to other Australian localities discussed in this section: A lower proportion of planktonic foraminifera and a higher abundance of agglutinated taxa were documented in the "lower Gearle Siltstone", that comprises the stratigraphically older parts of the section, in contrast to the upper part. Haig et al. (1996) identify nannofossil subzone CC8a and the *Sollasites falklandensis* Zone of the Southern Ocean calcareous nannofossil zonation (Pérez Panera, 2011 and references therein) and the marker *Muricohedbergella* (=*Hedbergella*) *planispira*, marking an early Albian age of the succession (Huber and Leckie, 2011). The lower to middle Albian benthic foraminiferal assemblages of the Gearle Siltstone can be correlated to *Ammobaculites* and *Marssonella* associations that were also identified at Site U1513.

5.1.2. Low- and northern high latitude records

The Albian foraminiferal record from the Australian continental margin faces some obstacles attempting global correlation as the record at Site U1513D illustrates a unique depositional environment spanning neritic to upper bathyal settings. A global correlation of the biostratigraphic data, biomarkers and zones of Site U1513 is a challenging effort, however, it is feasible on a large scale.

In the Tethyan realm, Giraldo Gómez et al. (2023) analysed an Albian succession in the Umbria Marche Basin in Italy (Fig. 10). They identified nannofossil zones NC 10a (equivalent to CC9) at Le Brecce and Monte Petrano within the Scaglia Bianca Formation. Giraldo-Gómez et al. (2023) document the planktonic foraminiferal *Thalmanninella appenninica* Zone, which includes OAE 1d. Coinciding with the termination of OAE 1d and overlying the *T. appenninica* zone, Giraldo-Gómez et al. (2023) record the lower Cenomanian *Thalmanninella globotruncanoides* Zone. Benthic markers for the Albian identified in the Italian sections that correlate to the Australian record include *Osangularia schloenbachi* and *Gavelinella intermedia*. The Albian $\delta^{13}C$ curve from the Umbria–Marche Basin exhibits a significant positive excursion associated with OAE 1d, defined as the interval between the initial $\delta^{13}C$ increase and the plateau of maximum values, that is expressing the key inflection points a, b and c (Giraldo-Gómez et al., 2023). The lower part of the excursion is characterized by black shale deposition, transitioning into marly limestones in the upper part, indicating changes in depositional conditions during the event (Fig. 10 nr.3, Giraldo-Gómez et al., 2023).

The studies by Scheibnerová (1976), Kochhann et al. (2013) and Bruno et al. (2020) on the South Atlantic Walvis Ridge Site 364 provide insights into Aptian/Albian nannofossil and planktonic foraminiferal stratigraphy (Fig. 10). Diverging from the nannofossil biostratigraphic results by Bruno et al. (2020), who place the succession of DSDP Site 364 entirely in the Albian, the study of Kochhann et al. (2013, 2023) documented shallow to deep neritic Aptian to Albian paleoenvironments during nannofossil zones CC8a, CC8b, CC9. From early to early late Albian, the *Gyroidinoides infracretaceus* association was recorded and in the late Albian, the *Kadriayina gradata* association of benthic foraminifera was identified. The latter association is characterized by a higher diversity of benthic foraminiferal species and yields potential marker species correlating to Site U1513, such as *Osangularia utaturensis* (in Scheibnerová, 1976, aform probably synonymous to *G. schloenbachi*), *Lingulogavelinella indica* (referred to as *Orithostella indica* in Kochhann et al., 2013) and pleurostomellids (*P. obtusa*; *P. subnodosa*). The benthic foraminiferal assemblages at Site 364 suggest a shift from dysoxic to more oxygenated settings during

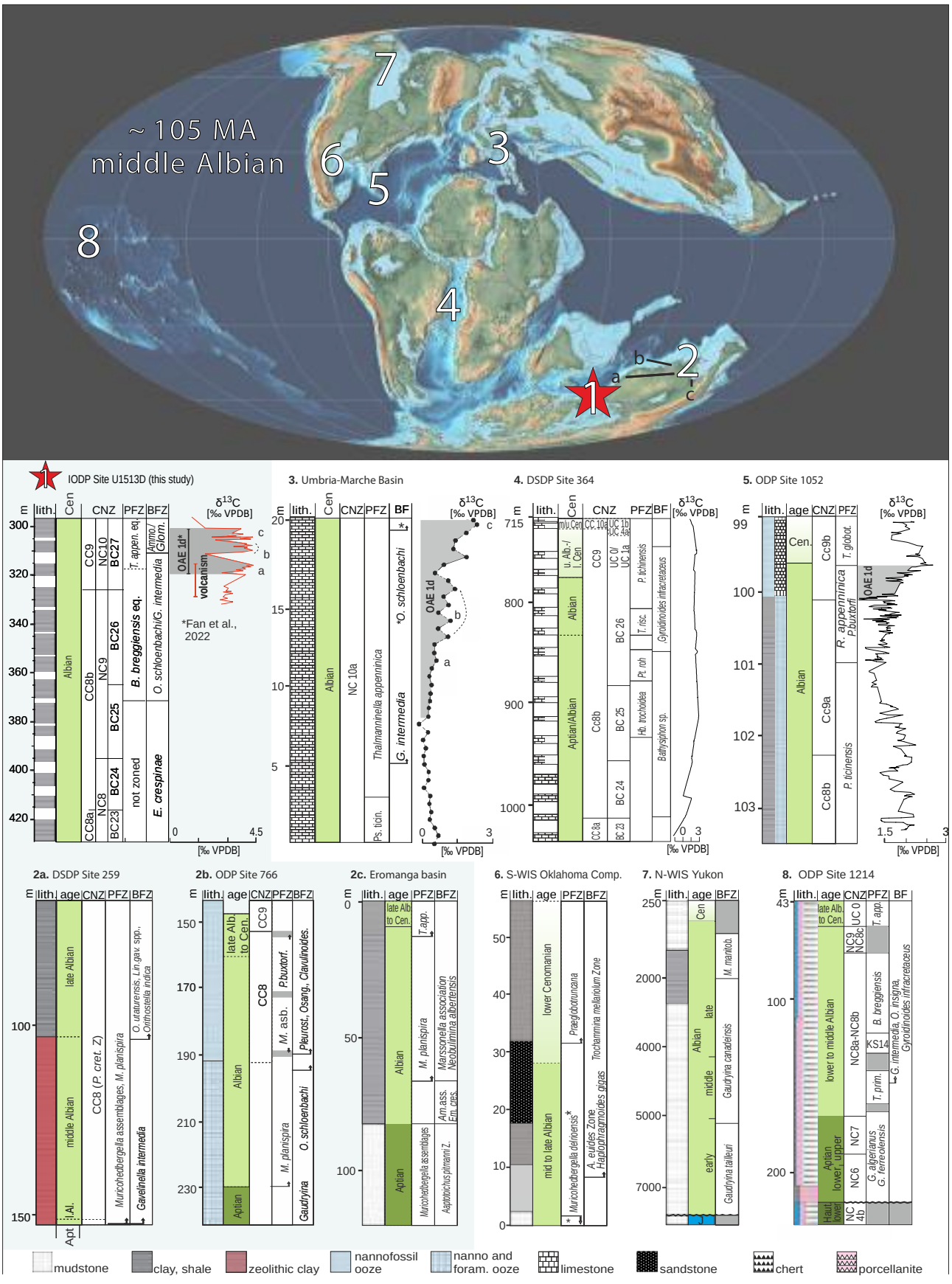

Fig. 10. Reconstruction of middle Albian paleogeography and simplified stratigraphy of selected localities (~105 MA, paleomap created with Gplates and based on Scotese, 2016). 1, locations of IODP Site U1513, the position of OAE 1d according to Fan et al. (2022) is shaded in grey. 2, Australian sections: 2a, DSDP Leg 27, Eastern Indian Ocean, Sites 259,260,

the Albian, a transition that is also reflected in lithological changes (Kochhann et al., 2014). The $\delta^{13}C$ curves of Site 364 (Fig. 10.4) show minor positive peaks during the Albian (Dummann et al., 2023).

Biostratigraphic markers used in the tropical western North Atlantic at Sites 1050 and 1052 (Blake Nose Plateau) span the nannofossil Zones CC9a and CC9b, which correlate to the *Pseudothalmanninella ticinensis* and *Thalmanninella appenninica* planktonic foraminiferal zones (Norris and Wilson, 1998; Petrizzo et al., 2008) (Fig. 10.5). Additionally, benthic foraminifera identified in Holbourn et al. (2001a) provide further evidence for Albian correlations in the Atlantic region. Benthic marker taxa found at Site U1513, including *Osangularia schloenbachi*, *Gavelinella intermedia*, and G. *cenomanica*, have also been documented in the South Atlantic, the western and eastern central Atlantic, the western Tethys, and the North Atlantic Holbourn et al. (2001a, Holbourn et al., 2001b.

The planktonic foraminiferal data assessed in the North Atlantic demonstrate a diversified assemblage compared to the southern high latitudes (Fig. 10). Western North Atlantic data from Sites 1050 and 1052 highlight increased levels of bioproductivity visible in nannofossil data before the collapse of ocean stratification that might have led to the onset of OAE1d (Watkins et al., 2005).

Few correlations can be found in the Western Interior Seaway (WIS) (Fig. 10). The southern and northern segments of the Albian WIS mostly illustrate shallow, marginal marine environments dominated by agglutinated foraminifera, whereas calcareous benthic are rare and planktonic foraminifera are virtually absent (documented in e.g., the Canadian section in Caldwell et al., 1978, New Mexico and Oklahoma, Scott et al., 2004, Fig. 10 nr.6 and 7).

The Albian benthic foraminiferal zonation in the Northern WIS (Fig. 10) frequently follows Caldwell et al. (1978), wherein the lower Albian is represented by the *Gaudryina nanushukensis*, the lower upper Albian by the *Haplophragmoides gigas* and the uppermost Albian by the *Miliammina manitobensis* benthic foraminiferal Zones. This zonational scheme correlates foraminiferal assemblages to palynomorph and, in particular, macrofossil stratigraphy (mostly ammonites and bivalves). The *Neogastroplites* ammonite Zone correlates tentatively to the upper part of the *H. gigas*, and the complete *M. manitobensis* Zone (Obradovich and Cobban, 1978). Among the most prominent markers for stratigraphic correlation is the Fish-Scale Marker Bed of the Colorado Shale, regionally marking the Albian/Cenomanian boundary (Leckie et al., 1992) and directly overlying the *M. manitobensis* Zone.

Stritch and Schröder-Adams (1999) and Schröder-Adams and Pedersen (2003) based the identification of the Albian sediments of Alberta and British Columbia, respectively, on correlations to adjacent rock formations and their inherent micro and macrofossil stratigraphy (Anan-Yorke and Stelck, 1978; Caldwell et al., 1993; Dixon, 1999), and documented the lower to middle Albian *Gaudryina nanushukensis* and the upper Albian *H. gigas* and *M. manitobensis* benthic foraminiferal Zones. The work of Quesnel et al. (2017) on the WIS in Yukon (Canada) documents a succession from a shelf to slope depositional environment to a marginal marine to non-marine environment, illustrating the *Gaudrayina tailleuri* Zone in the lower Albian and the *Gaudryina canadensis* Zone in the middle to upper Albian, succeeded by the *M. manitobensis* Zone (see Fig. 10.6). Like in the other northern WIS sections, the benthic foraminiferal assemblage is dominated by agglutinated taxa (i.e., *Gaudryina*, *Haplophragmoides*, *Miliammina*) and calcareous taxa are scarce (illustrated by few occurrences of *Gavelinella canadensis*, *G. avunensis*, *Anomalinoides* sp.), no planktonic taxa were recorded in this study (Fig. 10.7). The Southern WIS depicts an environment that was characterized by several transgressive-regressive settings during the Albian representing non marine, to estuarine and inner neritic depositional settings dominated by siliciclastic deposits (Scott et al., 2004) (Fig. 10). Well documented agglutinated benthic foraminifera that illustrate the *H. gigas* Zone (Scott et al., 2004) are recorded. A simplified documentation of successions at the Oklahoma Panhandle (Fig. 10.6) shows clear dominance of agglutinated, rarely documented calcareous benthic, and planktonic foraminifera virtually absent, only the rare occurrence of *Muricohedbergella* (=*Hedbergella*) *delrioensis* from the middle Albian is documented and nannofossils do not show a significant occurrence (Scott et al., 2004). Middle to upper Albian strata show inner shelf settings with *Ammobaculites* dominated assemblages (*Amobaculites euides* Zone). During the late Albian the southern WIS registers the return to marine conditions and towards the Albian/Cenomanian boundary the *Trochammina mellariolum* Zone shows increasing occurrences of planktonic foraminiferal taxa (*Praeglobotruncana*) (Eicher, 1965).

In conclusion, only a few benthic foraminiferal markers correlate between the southern Western Interior Seaway (Fig. 10.6) and Site 1513, and mostly at genus level. These correlations are primarily illustrated in nearshore shallow-water, marginal marine environments, characterized by predominantly agglutinated benthic foraminiferal communities with dominant elements such as *Haplophragmoides*, *Ammobaculites*, *Glomospira*, or *Trochammina*.

In the central Pacific Ocean ODP Sites 1207, 1214, and 1213 (Shatsky Rise), Giraldo-Gómez et al. (2022) document lower to middle Albian nannofossil zones CC8a and CC8b as well as the upper Albian zone NC9 (Fig. 10). Planktonic foraminiferal associations allow the identification of the *Ticinella primula* and the successive *Biticinella breggiensis* Zones, followed by the upper Albian *Thalmanninella appenninica* Zone. The biostratigraphic data of Shatsky Rise correlate only at genus level to some planktonic markers identified at Site U1513, the correlating benthic foraminiferal taxa include *G. intermedia* and *Osangularia insigna* (which is a form very similar and like *O. utaturensis* probably synonymous to the taxa *O. schloenbachi* according to Holbourn and Kaminski (1997).

263; 2b: ODP Leg 123, Cuvier Abyssal Plain; Carnarvon basin; Site 766; 2c, Eromanga basin, Hughenden 7 well) (Ludbrook, 1966; Scheibnerová, 1974; Moran, 1992; Haig 1992; Haig and Lynch, 1993; Haig et al., 1996). 3, Umbria-Marche basin, Italy (Giraldo-Gómez et al., 2023). 4, DSDP Leg 40, Southern Atlantic, Sites 363, 364 (Scheibnerová, 1976; Kochhann et al., 2014). 5, North Atlantic ODP Leg 171 Blake Nose Sites 1050, 1052, (Petrizzo et al., 2008; Wilson and Norris, 2001). 6, southern Western Interior Seaway (WIS) (Scott et al., 2004). 7, northern WIS (Quesnel et al., 2017). 8, North Pacific ODP Let 198, Sites 1207, 1213, and 1214 (Shatsky Rise), Giraldo-Gómez et al. (2023). See legend for lithologies in the bottom of Fig. 10. Abbreviations: m CCSF = meters Core Composite Depth Below Seafloor; Pf = planktonic foraminifera; Bf = benthic foraminifera; PFZ = planktonic foraminiferal Zone; BFZ = benthic foraminiferal Zone; CNZ = calcareous nannofossil Zone; PfN = planktonic foraminiferal number; BfN = benthic foraminiferal number; agBF = agglutinated benthic foraminifera; cBF = calcareous benthic foraminifera; m = metres; Cen = Cenomanian; Apt. = Aptian; WIS = Western Interior Seaway; *B. breggiensis* eq. = *Biticinella breggiensis* equivalent, and *T. appen* eq. = *Thalmanninella appenninica* equivalent zones. *T. prim* = *Ticinella primula*; *E. crespinae*/*Em. cres* = *Eomarssonella crespinae*; *O. schloenbachi* = *Osangularia schloenbachi*; *G. intermedia* = *Gavelinella intermedia*; *Ammo.* = *Ammodiscus*; *Glom.* = *Glomospira*; *H. trochoidea* = *Hedbergella trochoidea*; *M.* asb = *Muricohedbergella* assemblages; *P. buxtorf.* = *Planomalina buxtorfi*; *AM.* ass = *Ammobacculites* association; *A. euides* = *Ammobaculites euides*; *M. manitob.* = *Miliammina manitobensis*; *T. app.* = *Thalmanninella appeninnica*; *P. ticin.* = *P. ticinensis* = *Pseudothalmanninella ticinensis*; *T. globot.* = *Thalmanninella globotruncanoides*; *T. risc.* = *Ticinella rischi*; *Pt. roh.* = *Paraticinella rohri*; KS14 indicates the *T. praeticinensis* Subzone of the *Biticinella breggiensis* Zone, J = Jurassic, if present, significant excursions and points of inflection in ^{13}C signatures marked as a, b, c.

5.2. Paleoenvironmental comparisons

The late Albian transgression along the western Australian margin (e.g., Haig and Lynch, 1993; Haig et al., 1996; Campbell and Haig, 1999) resulted in a significant deepening of the depositional environment. Benthic foraminiferal assemblages at Site U1513 illustrate a shallow to inner neritic depositional environment below 370 m core depth, that is dominated by agglutinated taxa (Fig. 7). This assemblage shares similarities in foraminiferal biostratigraphy with the lower Albian assemblages documented by Campbell and Haig (1999) within the *Eomarssonella crespinae* Zone of the *Ammobaculites* association (Haig, 1979).

Above the 370 m mark (Fig. 7), a transgressive pulse, likely correlated with the global eustatic sea level highstand and the early Albian transgression documented in Northeast Australia (e.g., Critteden, 1987; Haig and Lynch, 1993; Villagómez et al., 1996; Jaillard et al., 2021; Nagendra and Reddy, 2021), led to rapid deepening, that is illustrated in changes in the benthic foraminiferal assemblage composition. Considering the depth-ranges of documented benthic foraminiferal species per sample, the increase from an inner neritic to an upper bathyal paleodepth between the base of the section and ~350 m CCSF, can be inferred applying the methodology used in Hohenegger (2005) and Wolfgring and Wagreich (2016). This transition is marked by the increase in the abundance of planktonic foraminifera and deeper-dwelling benthic taxa such as gavelinellids, *Pleurostomella* and *Osangularia* (Fig. 7).

The composition of the benthic foraminiferal fauna exhibits similarities to those documented in offshore localities described by Haig (1979) and Campbell and Haig (1999), specifically correlating with the *Gavelinella intermedia* Zone and the *Marssonella* association as identified by Haig (1979) (Fig. 10.2c).

Between ~350 and ~310 m CCSF (Fig. 7), a paleoenvironment displaying diverse calcareous benthic and few agglutinated species was documented, illustrating outer neritic to upper bathyal paleodepths.

The irregular occurrence and decline of planktonic and benthic foraminifera begins at approximately 320 m CCSF (Figs. 5, 7). Planktonic foraminifera exhibit a significantly higher abundance than average at 328.28 m CCSF, with overlying barren intervals and a substantial reduction in their overall presence are observed (Fig. 5). The highest abundance of calcareous benthic foraminifera occurs at 326.32 m CCSF, within an interval already barren of planktonic foraminifera. This offset between peaks in benthic and planktonic foraminiferal occurrence, followed by a drastic reduction in both groups up-section, likely reflects late Albian water-column instability and hydrographic changes in the Mentelle Basin. This pattern correlates with the onset of Oceanic Anoxic Event (OAE) 1d (Fig. 7).

Biostratigraphic and palaeoecological observations at Site U1513D were subsequently compared to the interval identified by Fan et al. (2022) as OAE 1d, revealing that key faunal shifts at Site U1513 align with the diagnostic geochemical signals of the event. The foraminiferal decline is not uniform but is characterized by near-barren intervals with alternating intervals documenting rare foraminiferal occurrences, particularly of opportunistic agglutinated taxa such as *Ammodiscus* and *Glomospira*, while calcareous benthic taxa that had diversified in the preceding upper Albian virtually disappear.

These faunal changes coincide with the positive $\delta^{13}C$ peaks, negative $\delta^{18}O$ shift, and elevated TOC contents reported in Fan et al. (2022) between 319 and 298 m CCSF, and are particularly visible in cores U1513D-25R to U1513D-27R supporting the interpretation that OAE 1d at southern high latitudes was accompanied by ecological stress and reduced bottom-water oxygenation. Importantly, these assemblage changes mirror similar disruptions observed in Tethyan and Atlantic records (e.g., Wilson and Norris, 2001; Giraldo-Gómez et al., 2023), confirming that OAE 1d imposed a global ecological signal that was particularly pronounced in high-latitude settings.

Changes in the abundance of calcareous foraminifera that lead to the dominance of dissolution resistant fauna composed by predominantly agglutinated taxa, can also frequently be attributed to shifts in watercolumn structure and bottom-water chemistry that promotes dissolution through shoaling of the carbonate compensation depth or increased acidification during hyperthermal events and OAEs (e.g., Petrizzo et al., 2022). Throughout the studied interval (pre-OAE1d), however, the sediment lithology remains uniform, illustrating predominantly claystone with no significant facies changes (see Figs. 2 and 3), meaning there are no notable lithologic shifts that could unambiguously account for assemblage changes. Benthic foraminiferal tests are consistently moderately preserved (Figs. 8 and 9), with no marked increase in dissolution, fragmentation throughout Site U1513D.

Facies changes may often coincide with environmental shifts and can influence microfossil assemblages. Furthermore, differential preservation (and the selective dissolution of thinner or more delicate tests) is known to distort the foraminiferal assemblage composition. The lack of variation in both lithology and preservation, as well as the minimal change in carbonate content at Site U1513, however, suggests that the entire fauna reflects an in-situ benthic community. After following a change in depositional environment comparable to that documented from other Austral sections (Haig, 1992; Haig and Lynch, 1993), above ~370 m CCSF the carbonate content steadily increases, reflecting a transition to a deeper, more open-marine environment (accompanied by the appearance of planktonic foraminifera and the change in dominant benthic foraminiferal association). This change corresponds with the shift from predominantly agglutinated to calcareous benthic foraminiferal assemblages and a parallel rise in planktonic foraminifera, indicating enhanced water-column stability and carbonate production. The uppermost part of the section, however, shows an abrupt decline in carbonate content that coincides with the position of OAE 1d (as defined in Fan et al., 2022).

Therefore, we assume that the documented changes in foraminiferal assemblages across this interval, aside from the OAE1d interval, most likely reflect genuine paleoenvironmental changes (e.g. shifts in productivity, oxygenation or water mass properties) rather than lithologic or taphonomic artifacts. Aside from the deepening in the lower section, assemblage and preservation changes appear only at the level of OAE 1d. We therefore interpret the shifts below OAE 1d as genuine ecological responses within an otherwise stable setting.

The position of OAE 1d, defined by Fan et al. (2022) on the basis of the $\delta^{13}C$ signature, is corroborated here by integrated foraminiferal and nannofossil stratigraphy. Within the depth range of 319–298 m CCSF, Site U1513 records the *Thalmanninella appenninica* Zone (cf. Petrizzo et al., 2008) together with the nannofossil marker species *Eiffellithus turriseiffelii* and *E. equibiramus*, which establish the base of CC09, NC10, and BC27 (Watkins et al., 2005). Both nannofossil abundance and preservation decline upwards through Zone CC09 (see Huber et al., 2019a, 2019b), consistent with stressed ecological conditions.

Coinciding with the decline in foraminifera and nannofossils observed in our assemblages, rare foraminiferal occurrences were reported in Haig (2005) from upper Albian radiolarian-rich black shales in Western Australia, further underscoring that foraminiferal decline and stressed marine ecosystems were widespread consequences of OAE 1d in the Austral realm. The disruption of

bottom and surface water stratification during OAE 1d, as documented at Blake Nose in the Atlantic by Norris et al. (1998), may be mirrored in the coupled reduction of planktonic and benthic foraminiferal abundance along the western Australian margin. Similar ecological stress patterns are reported from the western Tethys, where benthic foraminifera show repeated declines or disappear entirely in laminated shale intervals of the Pialli Level, reflecting rapid switches to hypoxic–anoxic bottom-water conditions (Giraldo-Gómez et al., 2023). These findings highlight that benthic faunas were particularly sensitive to short-term oxygen fluctuations, with opportunistic taxa (e.g., *Gyroidinoides* spp.) dominating under stressed conditions, whereas more diverse assemblages re-emerged only after the termination of OAE 1d. Moreover, the gradual decrease in the standing crop of foraminifera at Site U1513 extends beyond the top of OAE 1d, as defined by Fan et al. (2022), suggesting that the ecological effects of this event were protracted and not restricted to the strictly defined isotopic interval.

6. Conclusion

We examined IODP Hole U1513D between 429 and 297 m CCSF with the aim of investigating the planktonic and benthic foraminiferal and the nannofossil biostratigraphy of the Albian sediment in the southern high latitudes (Mentelle Basin, Australia). The investigation of nannofossils allow the identification of Zones CC8 to CC9. Due to limited resolution of the southern high latitude record during the Cretaceous, the planktonic foraminiferal assemblages documented at Site U1513 allow tentative identification of the *Biticinella breggiensis* equivalent and the *Thalmanninella appenninica* equivalent planktonic foraminifera zones. Benthic foraminiferal assemblages illustrate at least two different associations, the *Ammobacculites* and the *Marssonella* association, and three different benthic foraminiferal zones, the *Eomarssonella crespinae*, the *Osangularia schloenbachi*/*Gavelinella intermedia* and the *Ammodiscus*/*Glomospira* zones, all corresponding to specific environmental settings.

The *Eomarssonella crespinae* zone is dominated by agglutinated foraminiferal taxa illustrating a shallow bathymetric setting between ~430 and ~370 m CCSF at Site U1513 and planktonic foraminifera are absent. The overlying *Osangularia schloenbachi*/*Gavelinella intermedia* zone (between ~370 and 346 m CCSF) describes a late Albian transgressive environment, documenting the increasing abundance of calcareous benthic and planktonic foraminifera. The overlying interval from ~310 to 289 m CCSF is characterized by rapidly declining benthic and planktonic foraminiferal abundances, probably related to deteriorations in the ocean-climate system. According to Fan et al. (2022), the upper Albian record at Site U1513 documents the Oceanic Anoxic Event 1d within nannofossil zone CC9 and *T. appenninica* planktonic foraminiferal zone (~319–299m CCSF). The interval corresponding to OAE 1d at Site U1513 is marked by a pronounced decline in both planktonic and benthic foraminiferal abundance, with opportunistic agglutinated taxa prevailing. While not used to define the event, these assemblage changes corroborate the geochemical expression of OAE 1d and highlight the ecological sensitivity of southern high-latitude settings to comparatively short-lived perturbations in the late Albian.

CRediT authorship contribution statement

E. Wolfgring: Writing – review & editing. **M.R. Petrizzo:** Writing – review & editing. **D.K. Watkins:** Writing – review & editing.

Declaration of competing interest

The authors declare that they have no known competing financial interests or personal relationships that could have appeared to influence the work reported in this paper.

Acknowledgements

We thank Ottilia Szives for handling the editorial process and helpful remarks and Mark Leckie and two anonymous reviewers for their time, insightful comments and thoughtful suggestions that helped improve this manuscript. EW acknowledges support from the Brian J. O'Neill grant awarded by the Grzybowski Foundation. This research was funded in whole or in part by the Austrian Science Fund (FWF) 10.55776/J4444.

Data availability

Data will be made available on request.

References

Anan-Yorke, R., Stelck, C.R., 1978. Microfloras from Upper Albian Neogastroplites zone Sikanni Chief River, Northeastern British Columbia, Western and Arctic Canadian Biostratigraphy. In: Stelck, C.R., Chatterton, D.E. (Eds.), Geological Association of Canada, Special Paper, 15, pp. 473–493.

Bown, P.R., Rutledge, D., Crux, J.A., 1998. Lower Cretaceous. In: Bown, P.R. (Ed.), Calcareous Nannofossil Biostratigraphy. Kluwer Scientific, pp. 86–131.

Bralower, T.J., Leckie, R.M., Sliter, W.V., Thierstein, H.R., 1995. An integrated Cretaceous microfossil biostratigraphy. SEPM Special Publication 54, 65–79.

Bruno, M., Fauith, G., Watkins, D.K., Savian, J.F., 2020. Albian -Cenomanian calcareous nannofossils from DSDP Site 364 (Kwanza Basin, Angola): biostratigraphic and paleoceanographic implications for the South Atlantic. Cretaceous Research 109, 104377.

Caldwell, W.G.E., Diner, R., Eicher, D.L., Fowler, S.P., North, B.R., Stelck, C.R., von Holdt Wilhelm, L., 1978. Foraminiferal biostratigraphy and paleoecology of Cretaceous Eagle Sandstone and equivalent rocks, Saskatchewan and Manitoba. Geological Association of Canada Special Paper 18, 1–275.

Caldwell, W.G.E., Diner, R., Eicher, D.L., Fowler, S.P., North, B.R., Stelck, C.R., von Holdt Wilhelm, L., 1993. Foraminiferal biostratigraphy of Cretaceous marine cyclothems. In: Caldwell, W.G.E., Kauffman, E.G. (Eds.), Evolution of the Western Interior Basin: Geological Association of Canada Special Paper 39, pp. 477–520.

Campbell, R.J., Haig, D.W., 1999. Bathymetric change during Early Cretaceous intracratonic marine transgression across the northeastern Eromanga Basin, Australia. Cretaceous Research 20 (4), 403–446.

Critteden, S., 1987. The "Albian Transgression" in the southern North Sea Basin. Journal of Petroleum Geology 10 (4), 395–414.

Das Gupta, K., Saraswati, P., Kramar, U., Ravindran, C.N., Stüben, D., Berner, Z., 2007. Oxygen isotope composition of Albian-Turonian foraminifera from Cauvery Basin, India: evidence of warm sea-surface temperature. Journal of the Geological Society of India 69, 390–396.

Dixon, J., 1999. Mesozoic–Cenozoic stratigraphy of the Northern Interior Plains and Plateaux, Northwest Territories. Geological Survey of Canada, Bulletin 536, 1–56.

Dummann, W., Hofmann, P., Herrle, J.O., Frank, M., Wagner, T., 2023. The earlc opening of the Equatorial Atlantic gateway and the evolution of Cretaceous peak warming. Geology 51 (5), 476–480.

Dummann, W., Hofmann, P., Herrle, J.O., Wennrich, V., Wagner, T., 2021. A refined model of Early Cretaceous South Atlantic–Southern Ocean gateway evolution based on high-resolution data from DSDP Site 511 (Falkland Plateau). Palaeogeography, Palaeoclimatology, Palaeoecology 562, 110–113.

Eicher, D.L., 1965. Foraminifera and biostratigraphy of the Graneros Shale. Journal of Paleontology 39 (5), 875–909.

Fan, Q., Xu, Z., MacLeod, K.G., Brumsack, H.-J., Li, T., Chang, F., Wan, S., Riquier, L., Fu, D., Luan, Z., Duan, B., Chen, H., 2022. First record of oceanic anoxic event 1d at Southern high latitudes: sedimentary and geochemical evidence from International Ocean Discovery Program Expedition 369. Geophysical Research Letters 49, e2021GL09764.

Fauth, G., Kern, H.P., Villegas-Martín, J., et al., 2023. Early Aptian marine incursions in the interior of northeastern Brazil following the Gondwana breakup. Sci Rep 13, 6728. https://doi-org.uaccess.univie.ac.at/10.1038/s41598-023-32967-w.

Gibbons, A.D., Whittaker, J.M., Müller, R.D., 2013. The breakup of East Gondwana: assimilating constraints from Cretaceous ocean basins around India into a best-fit tectonic model. Journal of Geophysical Research: Solid Earth 118, 808–822. https://doi.org/10.1002/jgrb.50079.

Giraldo-Gómez, V.M., Petrizzo, M.R., Gambacorta, G., Bottini, C., Gilardoni, S.E., Erba, E., 2023. Benthic foraminifera across the Albian–Cenomanian transition

and their paleoceanographic significance during OAE1d in the western Tethys (Umbria–Marche Basin, Italy). Palaeogeography, Palaeoclimatology, Palaeoecology 631, 111820. https://doi-org.uaccess.univie.ac.at/10.1016/j.palaeo.2023.111820.

Giraldo-Gómez, V.M., Petrizzo, M.R., Erba, E., Bottini, C., 2022. Biostratigraphy, paleobathymetry and paleobiogeography of Lower Cretaceous benthic foraminifera from Shatsky Rise (ODP Leg 198) in the central Pacific Ocean. Cretaceous Research 138, 105283.

Haig, D.W., 1979. Global distribution patterns for mid-Cretaceous foraminiferids. Journal of Foraminiferal Research 9, 29–40.

Haig, D.W., 1992. Aptian-Albian foraminifers from Site 766, Cuvier Abyssal Plain, and comparison with coeval faunas from the Australian region. Proceedings of the Ocean Drilling Program, Scientific Results 132, 271–297.

Haig, D.W., Lynch, D.A., 1993. A late early Albian marine transgressive pulse over northeastern Australia, precursor to epeiric basin anoxia: foraminiferal evidence. Marine Micropaleontology 22, 311–362.

Haig, D.W., 2005. Foraminiferal evidence for inner neritic deposition of Lower Cretaceous (Upper Aptian) radiolarian-rich black shales on the Western Australian margin. Journal of Micropalaeontology 24 (1), 55–75. https://doi.org/10.1144/jm.24.1.55.

Haig, D.W., Mory, A.J., Dixon, M., Backhouse, J., Campbell, R.J., Ghori, K.A.R., Howe, R., Morris, P.A., 2004. GS WA Boologooro 1 well completion report (interpretive), southern Carnarvon Basin, Western Australia. Record of the Geological Survey of Western Australia 2004 (4), 106.

Haig, D.W., Watkins, D.K., Ellis, G., 1996. Mid-Cretaceous calcareous and siliceous microfossils from the basal Gearle Siltstone, Giralia Anticline, Southern Carnarvon Basin. Alcheringa 41–68.

Harry, D.L., Tejada, M.L.G., Lee, E.Y., Wolfgring, E., Wainman, C.C., Brumsack, H.-J., Schnetger, B., Kimura, J.-I., Riquier, L., Borissova, I., Hobbs, R.W., Jiang, T., Li, Y., Maritati, A., Martinez, M., Richter, C., Tagliaro, G., White, L.T., 2020. Evolution of the Southwest Australian rifted continental margin during breakup of East Gondwana: results from International Ocean Discovery Program Expedition 369. Geochemistry, Geophysics, Geosystems 21. https://doi.org/10.1029/2020GC009144.

Hohenegger, J., 2005. Estimation of environmental paleogradient values based on presence and absence data of benthic foraminifera. Palaeogeography, Palaeoclimatology, Palaeoecology 217 (1–2), 115–130.

Holbourn, A.E.L., Henderson, A., MacLeod, N., 2013. Atlas of Benthic Foraminifera. https://doi.org/10.1002/9781118452493.

Holbourn, A.E.L., Kaminski, M.A., 1995. Lower Cretaceous benthic foraminifera from DSDP Site 263: micropalaeontological constraints for the early evolution of the Indian Ocean. Marine Micropaleontology 26, 425–460.

Holbourn, A.E.L., Kaminski, M.A., 1997. Lower Cretaceous deep-water benthic Foraminifera of the Indian Ocean. Grzybowski Foundation Special Publication 4, 172.

Holbourn, A.E.L., Kuhnt, W., Erbacher, J., 2001a. Benthic foraminifers from lower Albian black shales (Site 1049, ODP Leg 171): evidence for a non "uniformitarian" record. Journal of Foraminiferal Research 31 (1), 60–74.

Holbourn, A.E.L., Kuhnt, W., Soeding, E., 2001b. Atlantic paleobathymetry, paleoproductivity and paleocirculation in the late Albian: the benthic foraminiferal record. Palaeogeography, Palaeoclimatology, Palaeoecology 170, 171–196.

Huber, B.T., Hodell, D.A., Hamilton, C.P., 1995. Middle–Late Cretaceous climate of the southern high latitudes: stable isotopic evidence for minimal equator-to-pole thermal gradients. Geological Society of America Bulletin 107, 1164–1191.

Huber, B.T., Hobbs, R.W., Bogus, K.A., Batenburg, S.J., Brumsack, H.-J., do Monte Guerra, R., Edgar, K.M., Edvardsen, T., Garcia Tejada, M.L., Harry, D.L., Hasegawa, T., Haynes, S.J., Jiang, T., Jones, M.M., Kuroda, J., Lee, E.Y., Li, Y.-X., MacLeod, K.G., Maritati, A., Martinez, M., O'Connor, L.K., Petrizzo, M.R., Quan, T.M., Richter, C., Riquier, L., Tagliaro, G.T., Wainman, C.C., Watkins, D.K., White, L.T., Wolfgring, E., Xu, Z., 2019a. Expedition 369 methods. In: Hobbs, R.W., Huber, B.T., Bogus, K.A., the Expedition 369 Scientists (Eds.), Australia Cretaceous Climate and Tectonics, Proceedings of the International Ocean Discovery Program, 369. International Ocean Discovery Program, College Station, TX. https://doi.org/10.14379/iodp.proc.369.102.2019.

Huber, B.T., Hobbs, R.W., Bogus, K.A., Batenburg, S.J., Brumsack, H.-J., do Monte Guerra, R., Edgar, K.M., Edvardsen, T., Garcia Tejada, M.L., Harry, D.L., Hasegawa, T., Haynes, S.J., Jiang, T., Jones, M.M., Kuroda, J., Lee, E.Y., Li, Y.-X., MacLeod, K.G., Maritati, A., Martinez, M., O'Connor, L.K., Petrizzo, M.R., Quan, T.M., Richter, C., Riquier, L., Tagliaro, G.T., Wainman, C.C., Watkins, D.K., White, L.T., Wolfgring, E., Xu, Z., 2019b. Site U1513. In: Hobbs, R.W., Huber, B.T., Bogus, K.A., the Expedition 369 Scientists (Eds.), Australia Cretaceous Climate and Tectonics, Proceedings of the International Ocean Discovery Program, 369. International Ocean Discovery Program, College Station, TX. https://doi.org/10.14379/iodp.proc.369.104.2019.

Huber, B.T., Leckie, R.M., 2011. Planktic foraminiferal species turnover across deep-sea Aptian/Albian boundary sections. Journal of Foraminiferal Research 41 (1), 53–95.

Huber, B.T., Petrizzo, M.R., Young, J.R., Falzoni, F., Gilardoni, S.E., Bown, P.R., Wade, B.S., 2016. Pforams@mikrotax: a new online taxonomic database for planktonic foraminifera. Micropaleontology 62 (6), 429–438.

Jaillard, E., Chihaoui, A., Latil, J.L., et al., 2021. Sequences, discontinuities and water stratification in a low-energy ramp: the Early Albian sedimentation in central Tunisia. International Journal of Earth Sciences 110, 263–285. https://doi.org/10.1007/s00531-020-01951-4.

Kaminski, M.A., Boersma, E., Tyszka, J., Holbourn, A.E.L., 1995. Response of deep-water agglutinated foraminifera to dysoxic conditions in the California Borderland basins. In: Proceedings of the Fourth International Workshop Agglutinated Foraminifera Sept. 12-19 1993. Grzybowski Foundation Special Publication, 3, pp. 131–140.

Kanungo, S., Bown, P., Gale, A., 2020. Cretaceous (Albian-Turonian) calcareous nannofossil biostratigraphy of the onshore Cauvery Basin, southeastern India. Cretaceous Research 118 (5), 104644.

Kochhann, K.G.D., Koutsoukos, E.A.M., Fauth, G., 2014. Aptian–Albian benthic foraminifera from DSDP Site 364 (offshore Angola): a paleoenvironmental and paleobiogeographic appraisal. Cretaceous Research 48, 1–11.

Kochhann, K.G.D., Koutsoukos, E.A.M., Fauth, G., Sial, A.N., 2013. Aptian-Albian planktic foraminifera from DSDP Site 364 (offshore Angola): biostratigraphy, paleoecology and paleoceanographic significance. Journal of Foraminiferal Research 43, 443–463.

Kochhann, K.G.D., Huber, B.T., Holbourn, A.E., Kuhnt, W., 2023. Benthic Foraminiferal response to the Aptian-Albian carbon cycle perturbation in the Atlantic Ocean. Journal of Foraminiferal Research 53 (3), 214–225.

Koutsoukos, E.A.M., Hart, M.B., 1990. Cretaceous foraminiferal morphogroup distribution patterns, palaeocommunities and trophic structures: a case study from the Sergipe Basin, Brazil. Transactions of the Royal Society of Edinburgh: Earth Sciences 81, 221–246.

Koutsoukos, E.A.M., 1989 (Ph.D. thesis). Mid- to Late Cretaceous Microbiostratigraphy, Palaeo-ecology and Paleogeography of the Sergipe Basin, Northeastern Brazil, Vols 1 & 2. University of Plymouth, United Kingdom, p. 886. Open Access repository at: http://hdl.handle.net/10026.1/2016.

Krasheninnikov, V.A., Basov, I.A., 1983. Stratigraphy of Cretaceous sediments of the Falkland Plateau based on planktonic foraminifers, Deep Sea Drilling Project, Leg 71. In: Ludwig, W.F., Krasheninnikov, V.A., et al. (Eds.), Initial Reports of the Deep Sea Drilling Project, 71. U.S. Government Print Office, Washington, pp. 789–820. https://doi.org/10.2973/dsdp.proc.71.129.1983.

Leckie, M.R., 1990. Middle Cretaceous planktonic foraminifers of the Antarctic margin: hole 693A, ODP LEG 1131. In: Proceedings of the Ocean Drilling Program, Scientific Results, 113, pp. 319–324.

Leckie, D.A., Singh, C., Bloch, J., Wilson, M., Wall, J., 1992. An anoxic event at the Albian-Cenomanian boundary: the Fish Scale Marker Bed, northern Alberta, Canada. Palaeogeography, Palaeoclimatology, Palaeoecology 92 (1–2), 139–166.

Lee, E.Y., Wolfgring, E., Tejada, M.L.G., Harry, D.L., Wainman, C.C., Chun, S.S., Schnetger, B., Brumsack, H.-J., Maritati, A., Martinez, M., Richter, C., Li, Y.-X., Riquier, L., MacLeod, K.G., Waller, T.R., Borissova, I., Petrizzo, M.R., Huber, B.T., Kim, Y., 2020. Early Cretaceous subsidence of the Naturaliste Plateau defined by a new record of volcaniclastic-rich sequence at IODP Site U1513. Gondwana Research 82, 1–11. https://doi.org/10.1016/j.gr.2019.12.007.

Ludbrook, N.H., 1966. Cretaceous biostratigraphy of the Great Artesian Basin in South Australia. Bulletin of the Geological Survey of South Australia 40, 1–223.

Malumián, N., Nanez, C., 2002. Los Foraminiferos de la Provincia de Santa Cruz: Su significado geologico y paleoambiental. In: Haller, M.J. (Ed.), XV Congreso Geológico Argentino (El Calafate, 2002), Geología y Recursos Naturales de Santa Cruz, Relatorio, II-8, pp. 1–13.

Malumián, N., 1982. Caracterfsticas bioestratigráficas de las asociaciones foraminfferológicas de la República Argentina. In: 5th Congreso Latinoamericano de Geología, Actas 1, pp. 779–790.

Malumián, N., Ramos, V., 1984. Magmatic intervals, transgression-regression cycles and oceanic events in the Cretaceous and Tertiary of southern South America. Earth and Planetary Science Letter 67, 228–237.

Moran, M.J., 1992. Biostratigraphy of Upper Cretaceous and Paleocene calcareous nannofossils from Leg 123, northeastern Indian Ocean. In: Gradstein, F.M., Ludden, J.N., et al. (Eds.), Proceedings of the Ocean Drilling Program, Scientific Results, 123. Ocean Drilling Program, College Station, TX, pp. 381–405.

Murray, J.W., Alve, E., Jones, R.W., 2011. A new look at modern agglutinated benthic foraminiferal morphogroups: their value in palaeoecological interpretation. Palaeogeography, Palaeoclimatology, Palaeoecology 309, 229–241.

Murray, J.W., Alve, E., 2000. Major aspects of foraminiferal variability (standing crop and biomass) on a monthly scale in an intertidal zone. Journal of Foraminiferal Research 30 (3), 177–191.

Nagendra, R., Reddy, N.A., 2021. Litho-Biostratigraphy and depositional environment of Albian-Maastrichtian sedimentary succession of Cauvery Basin in Ariyalur area. In: Banerjee, S., Sarkar, S. (Eds.), Mesozoic Stratigraphy of India, Society of Earth Scientists Series. Springer, Cham. https://doi.org/10.1007/978-3-030-71370-6_19.

Norris, R.D., Kroon, D., Klaus, A., Shipboard Scientific Party, 1998. Explanatory notes. In: Norris, R.D., Kroon, D., Klaus, A., Shipboard Scientific Party (Eds.), Proceedings of the Ocean Drilling Program Initial Reports, v. 160, pp. 11–42.

Norris, R.D., Wilson, P.A., 1998. Low-latitude sea- surface temperatures for the mid-Cretaceous and the evolution of planktic foraminifera. Geology 26, 823–826.

Nyong, E.E., Olsson, R.K., 1984. A paleoslope model of Campanian-lower Maestrichtian foraminifera in the North American Basin and adjacent continental margin. Marine Micropaleontology 8 (188/84), 437–477.

Obradovich, J.D., Cobban, W.A., 1978. K-Ar dating of the Albian. U.S. Geological Survey Professional Paper 1100 191 [GD I 19.16:1100].

Perch-Nielsen, K., 1985. Mesozoic calcareous nannofossils. In: Bolli, H.M., Saunders, J.B., Perch-Nielsen, K. (Eds.), Plankton Stratigraphy. Cambridge University Press, Cambridge, pp. 329–426.

Pérez Panera, J.P., 2011. The calcareous nannofossil Sollasites falklandensis (Coccolithophyceae) and its biostratigraphic and Palaeoceanographic importance in the Albian of Austral Basin, Argentina. Cretaceous Research 32 (6), 723–737.

Pérez Panera, J.P., 2012. Nanofósiles calcáreos y bioestratigrafía del cretácico del sudeste de la Cuenca Austral, Patagonia, Argentina. Ameghiniana 49 (2), 137–163.
Petrizzo, M.R., Huber, B.T., 2006. Biostratigraphy and taxonomy of late Albian planktonic foraminifera from ODP Leg 171B (western North Atlantic Ocean). Journal of Foraminiferal Research 36, 165–189.
Petrizzo, M.R., Gilardoni, S.E., 2020. Planktonic foraminiferal biostratigraphy of the Late Albian-Cenomanian pelagic sequences from the Umbria-Marche basin (Central Italy) and the Mazagan Plateau (Northeast Atlantic Ocean). Rivista Italiana di Paleontologia e Stratigrafia 126 (3), 865–904.
Petrizzo, M.R., Huber, B.T., Gale, A.S., Barchetta, A., Jenkyns, H.C., 2012. Abrupt planktic foraminiferal turnover across the Niveau Kilian at Col de Pré-Guittard (Vocontian Basin, southeast France): new criteria for defining the Aptian/Albian boundary. Newsletters on Stratigraphy 45 (1), 55–74.
Petrizzo, M.R., Huber, B.T., Wilson, P.A., MacLeod, K.G., 2008. Late Albian paleoceanography of the western subtropical North Atlantic. Paleoceanography and Paleoclimatology 23. https://doi.org/10.1029/2007PA001517.
Petrizzo, M.R., Amaglio, G., Watkins, D.K., MacLeod, K.G., Huber, B.T., Hasegawa, T., Wolfgring, E., 2022. Biotic and paleoceanographic changes across the Late Cretaceous Oceanic Anoxic Event 2 in the southern high latitudes (IODP sites U1513 and U1516, SE Indian Ocean). Paleoceanography and Paleoclimatology 37 (9), e2022PA004474. https://doi.org/10.1029/2022PA004474.
Premoli Silva, I., Sliter, W.V., 1995. Cretaceous Planktonic Foraminiferal Biostatigraphy and Evolutionary Trends from the Bottaccione Section, Gubbio, Italy. Paleontographica Italica 82, 1–89.
Quesnel, A., Schröder-Adams, C.J., Davis, W.J., 2017. Cretaceous (Albian to Cenomanian) biostratigraphic, paleogeographic and paleoenvironmental reconstruction of the northern Western Interior Sea: Yukon, Canada. Palaeogeography, Palaeoclimatology, Palaeoecology 468, 453–472.
Robaszynski, F., Caron, M., 1995. Foraminifers planktonique du Crétacé. Bulletin Society Geological of France 166, 681–698.
Scheibnerová, V., 1974. Aptian-Albian benthonic foraminifera from DSDP Leg 27 Sites 256-260 and 263, eastern Indian Ocean. Initial Reports of DSDP 27, 697–741. Washington.
Scheibnerová, V., 1976. Cretaceous Foraminifera of the Great Australian Basin. Memoirs of the Geological Survey of New South Wales. Palaeontology 17, 1–277.
Scheibnerová, V., 1981. Palaeogeographical implications of Cretaceous Benthic Foraminifera recovered by the Deep Sea Drilling project in the Western South Atlantic Ocean. Cretaceous Research 2 (1), 1–18.
Schröder-Adams, C.J., Pedersen, P.K., 2003. Litho- and biofacies analyses of the Buckinghorse Formation: the Albian Western Interior Sea in northeastern British Columbia (Canada). Bulettin of Canadian Petroleum Geology 51 (3), 234–252.
Scotese, C.R., 2016. PALEOMAP PaleoAtlas for GPlates and the PaleoData Plotter Program. PALEOMAP Project. http://www.earthbyte.org/paleomap, paleoatlasforgplates/.
Scott, R., Holbrook, J., Oboh-Ikuenobe, F., Evetts, M.J., Benson, D.G., Kues, B., 2004. Middle Cretaceous stratigraphy, Southern Western Interior Seaway, New Mexico and Oklahoma. Mountain Geologist 41, 33–61.
Stritch, R.A., Schröder-Adams, C.J., 1999. Foraminiferal response to Albian relative sea-level changes in northwestern and central Alberta, Canada. Canadian Journal of Earth Sciences 36 (10), 1617–1643.
Tewari, A., Hart, M.B., Watkinson, M.P., 1996. Foraminiferal recovery after the mid-Cretaceous oceanic anoxic events (OAEs) in the Cauvery Basin, southeast India. Geological Society London Special Publications 102, 237–244. https://doi.org/10.1144/GSL.SP.1996.001.01.17.
Venkatachalapathy, R., Ragothaman, V., 1995. A foraminiferal zonal scheme for the mid-Cretaceous sediments of the Cauvery Basin, India. Cretaceous Research 16, 415–533.
Villagómez, R., Jaillard, E., Bulot, L., Rivadeneira, M., Vera, R., 1996. The Aptian-Late Albian Marine transgression in the Oriente Basin of Ecuador. In: Third ISAG, 521-524, St. Malo (France), 17-19.9.1996.
Wainman, C.C., Borissova, I., Harry, D.L., Hobbs, R.W., Mantle, D.J., Mariati, A., Lee, E.Y., the Expedition 369 Scientists, 2019. Evidence for non-marine Jurassic to earliest Cretaceous sediments in the pre-breakup section of the Mentelle Basin, southwestern Australia. Australian Journal of Earth Sciences. https://doi.org/10.1080/08120099.2019.1627581.
Wainman, C.C., Tagliaro, G., Jones, M.M., Charles, A.J., Hall, T., White, L.T., Bogus, K.A., Wolfgring, E., O'Connor, L.K., McCabe, P.J., Holford, S.P., 2020. The sedimentological evolution and petroleum potential of a very thick Upper Cretaceous marine mudstone succession from the southern high latitudes—a case study from the Bight Basin, Australia. Marine and Petroleum Geology 118, 104441. https://doi.org/10.1016/j.marpetgeo.2020.104441.
Watkins, D.K., Cooper, M.J., Wilson, P.A., 2005. Calcareous nannoplankton response to late Albian oceanic anoxic event 1d in the western North Atlantic. Paleoceanography and Paleoclimatology 20, 2. https://doi.org/10.1029/2004PA001097.
White, L.T., Forster, M.A., Tanner, D., Tejada, M.L.G., Hobbs, R., IODP Expedition 369 Science Party, 2020. The timing of magmatism and subsequent alteration of basaltic rocks cored at the base of IODP Site U1513. Preprint, Earth ArXiv. https://eartharxiv.org/repository/view/279/.
White, L.T., Gibson, G.M., Lister, G.S., 2013. A reassessment of paleogeographic reconstructions of eastern Gondwana: bringing geology back into the equation. Gondwana Research 24, 984–998. https://doi.org/10.1016/j.gr.2013.06.009.
Wignall, P.B., Bond, D.P.G., Kuwahara, K., Kakuwa, Y., Newton, R.J., Poulton, S.W., 2010. An 80 million year oceanic redox history from Permian to Jurassic pelagic sediments of the Mino-Tamba terrane, SW Japan, and the origin of four mass extinctions. Global and Planetary Change 71, 109–123. https://doi.org/10.1016/j.gloplacha.2010.01.022.
Wilson, P.A., Norris, R.D., 2001. Warm tropical ocean surface and global anoxia during the mid-Cretaceous period. Nature 412 (6845), 425–429. https://doi.org/10.1038/35086553.
Wolfgring, E., Wagreich, M., 2016. A quantitative look on northwestern Tethyan foraminiferal assemblages, Campanian Niertental Formation, Austria. PeerJ 4, e1757. https://doi.org/10.7717/peerj.1757.
Wolfgring, E., Petrizzo, M.R., 2024. Upper Cretaceous benthic foraminiferal biostratigraphy at IODP Site U1513, Mentelle Basin, SE Indian Ocean. Micropaleontology 70 (1), 43–59. https://doi.org/10.1016/j.cretres.2023.105555.
Wolfgring, E., Amaglio, G., Petrizzo, M.R., 2023. Cretaceous southern high latitude benthic foraminiferal assemblages during OAE 2 at IODP Site U1516, Mentelle Basin, Indian Ocean. Cretaceous Research 148, 105555.

Appendix A. Supplementary data

Supplementary data to this article can be found online at https://doi.org/10.1016/j.cretres.2026.106355.

Appendix 1

List of foraminiferal taxa documented in the Albian of Site U1513

Planktonic foraminifera:

Clavihedbergella simplex	(Morrow, 1934)
Laeviella bentonensis	(Morrow, 1934)
Laeviella sp.	
Microhedbergella albiana	(Boudagher-Fadel et al., 1996)
Microhedbergella praeplanispira	Huber & Leckie, 2011
Microhedbergella pseudodelrioensis	Huber & Leckie, 2011
Microhedbergella sp.	
Muricohedbergella delrioensis	(Carsey, 1926)
Muricohedbergella sp.	
Protoheterohelix sp.	
Ticinella madecassiana	Sigal, 1966
Ticinella primula	Luterbacher, in Renz et al., 1963
Whiteinella baltica	Douglas & Rankin, 1969

Benthic foraminifera:

Aaptotoichus sp.	
Ammodiscus cretaceus	Reuss, 1845
Ammodiscus peruvianus	Berry, 1928
Ammodiscus sp.	
Ammogloborotalia abrupta	(Geroch, 1966)
Astacolus gratus	(Reuss, 1863)
Astacolus sp.	
Bulbobaculites problematicus	(Neagu, 1962)
Buzasina cf. *antarctica*	Kaminski, Wolfgring & Waśkowska, 2020
Conorboides claytonensis	Ludbrook, 1966
Conorotalites sp.	
Dentalina communis	(d'Orbigny, 1826)
Dentalina sp.	
Discorbis sp.	
Eggerellina sp.	
Ellipsodimorphina sp.	
Ellipsoidella cuneiformis	Fuchs, 1967
Eomarssonella crespinae	(Ludbrook, 1966)
Fissurina sp.	
Frondicularia extensa	Morrow, 1934
Gavelinella cenomanica	(Brotzen, 1945)
Gavelinella crespinae	Scheibnerová, 1976
Gavelinella intermedia	(Berthelin, 1880)
Gavelinella sp.	
Globorotalites sp.	
Glomospira charoides	(Jones & Parker, 1860)
Glomospira diffundens	Cushman & Renz, 1946
Glomospira gordialis	(Jones & Parker, 1860)
Glomospira sp.	
Glomospirella sp.	
Gyroidina sp. *1*	(Scheibnerová, 1975, fig. 105)
Gyroidinoides lenticulus	(Reuss, 1845)
Gyroidinoides primitivus	(Hofker, 1957)
Gyroidinoides quadratus	(Cushman & Church, 1929)
Gyroidinoides sp.	
Gyroidinoides umbilicatus	(d'Orbigny, 1840)
Haplophragmoides sp.	
Haplophragmoides walteri	(Grzybowski, 1898)
Haplopphragmoides antarcticus	Wolfgring, Kaminski & Waśkowska, 2023
Kalampopsis grzybowskii	(Dylążanka, 1923)
Labrospira sp.	
Laevidentalina catenula	(Reuss, 1860)
Laevidentalina linearis	(Roemer, 1841)
Laevientalina elegans (plexus*: L.elegans, L. gracilis*)	(d'Orbigny, 1846)
Lagena striata	(d'Orbigny, 1839)
Lenticulina bayrocki	Mellon & Wall, 1956
Lenticulina gaultina	(Berthelin, 1880)
Lenticulina muensteri	(Roemer, 1839)
Lenticulina secans (ornamented)	(Reuss, 1860)
Lenticulina sp.	
Lenticulina sp. cf. *warregoensis*	Crespin, 1944
Lenticuluna macrodisca	(Reuss, 1863)
Lingulogavelinella sp.	
Lingulogavelinella albiensis	Malapris, 1965
Lingulogavelinella indica	(Scheibnerová, 1974)
Lingulogavelinells frankei	(Bykova, 1953)
Marginulina sp.	
Marginulinopsis arimensis	Ludbrook, 1966
Marginulinopsis pristipellis	Ludbrook, 1966
Marginulinopsis gracilissima	(Reuss, 1863)
Marginuliopsis tilchae	Ludbrook, 1966
Nodosaria limbata	d'Orbigny, 1840
Nodosaria sp.	
Oolina laevigata	d'Orbigny, 1839
Oolina sp.	
Osangularia schloenbachi	(Reuss, 1863)
Osangularia sp.	
Planularia complanata	(Reuss, 1845)
Planularia sp.1 (broad, not *complanata*)	
Pleurostomella obtusa	Berthelin, 1880
Pleurostomella sp.	
Pleurostomella subnodosa	(Reuss, 1851)
Pleurostomella velascoensis	Cushman, 1926
Praebulimina sp.	
Pseudonodosaria sp.	
Pyramidulina sp.	

(*continued*)

Pyrulina sp.	
Ramulina sp.	
Recurvoides sp.	
Reinholdella ? sp.	
Rhabdammina sp.	
Saracenaria elita	Ludbrook, 1966
Saracenaria sp.	
Scutuloris sp.	
Spiroplectammina sp.	Cushman, 1927
Stiliostomella sp.	
Textularia sp	
Tristix excavata	(Reuss, 1863)
Tristix sp	
Trochammina minuta	Crespin, 1953
Vaginulina reussi	Agalarova, 1951
Vaginulina sp.	
Valvulineria infrequens	Morrow, A. L. 1934
Valvulineria sp.	

Calcareous nannofossils:

Assipetra terebrondentatrius	Covington & Wise, 1987
Axopodorhabdus biramiculatus	(Black) Wind and Wise 1977
Axopodorhabdus dietzmannii	(Reinhardt, 1965) Wind & Wise, 1983
Biscutum aura	Brace & Watkins (2014)
Biscutum ubiquens	(Brace and Watkins, 2014)
Braarudosphaera regularis	Black, 1973
Broinsonia galloisii	(Black, 1973) Bown in Kennedy et al., 2000
Bukrylithus ambiguus	Black, 1971
Calciosolenia fossilis	(Deflandre in Deflandre & Fert, 1954) Bown in Kennedy et al., 2000
Ceratolithina bicornuta	Perch-Nielsen, 1988
Ceratolithina copis	Burnett, 1997
Ceratolithina cruxii	Perch-Nielsen, 1988
Chiastozygus platyrhethus	Hill, 1976
Chiastozygus tenuis	Black, 1971
Corollithion signum	Stradner, 1963
Cretarhabdus conicus	Bramlette & Martini, 1964
Cretarhabdus crenulatus	Worsley, 1971
Cretarhabdus striatus	(Stradner, 1963; Black, 1976); Stradner, 1963
Cretarhabdus surirella	(Deflandre & Fert, 1954)
Cribrosphaerella ehrenbergii	(Arkhangelsky, 1912) Deflandre in Piveteau, 1952
Crucicribrum anglicum	Black, 1973
Cyclagelosphaera margerelii	Noël, 1965
Cyclagelosphaera reinhardtii	(Perch-Nielsen, 1968) Romein, 1977
Cyclagelosphaera rotaclypeata	Bukry, 1969
Discorhabdoides filiformis	Lambert 1987
Discorhabdus ignotus	(Górka, 1957) Perch-Nielsen, 1968
Eiffellithus casulus	Shamrock in Shamrock & Watkins, 2009
Eiffellithus equibiramus	Watkins & Bergen, 2003
Eiffellithus monechiae	Crux, 1991
Eiffellithus paragogus	Gartner, in Robaszynski et al., 1993.
Eiffellithus parvus	Watkins & Bergen, 2003
Eiffellithus praestigium	Watkins & Bergen, 2003
Eiffellithus turriseiffelii	(Deflandre in ; Reinhardt, 1965
Eprolithus floralis	(Stradner, 1962) Stover, 1966
Flabellites oblongus	(Bukry, 1969) Crux in Crux et al., 1982
Gaarderella granulifera	Black, 1973
Gartnerago ponticula	Bown & Hampton in Bown, 2005
Gartnerago praeobliquum	Jakubowski, 1986
Gartnerago stenostaurion	(Hill, 1976)
Glaukolithus bicrescentricus	(Stover, 1966) Burnett in Gale et al., 1996
Glaukolithus diplogrammus	(Deflandre, 1954)
Gorkaea operio	Varol & Girgis, 1994
Grantarhabdus coronadventis	(Reinhardt, 1966) Grün in Grün & Allemann, 1975
Grantarhabdus coronadventis (large)	(Reinhardt, 1966) Grün in Grün & Allemann, 1975
Grantarhabdus coronadventis (small)	(Reinhardt, 1966) Grün in Grün & Allemann, 1975
Haqius circumradiatus	(Stover, 1966) Roth, 1978
Hayesites albiensis	Manivit, 1971
Helenea chiastia	Worsley, 1971
Helicolithus compactus	(Bukry, 1969) Varol & Girgis, 1994
Helicolithus trabeculatus (<7 um)	(Górka, 1957) Verbeek, 1977
Laguncula dorotheae	Black, 1971
Lapideacassis cornuta	(Forchheimer & Stradner, 1973) Wind & Wise in Wise & Wind, 1977

(*continued on next page*)

(*continued*)

Lapideacassis mariae	Black, 1971
Lithraphidites carniolensis	Deflandre, 1963
Manivitella pemmatoidea	(Deflandre in Manivit, 1965) Thierstein, 1971
Octocyclus magnus	Black, 1972
Octocyclus reinhardtii	(Bukry, 1969) Wind & Wise in Wise & Wind, 1977
Pickelhaube furtiva	(Roth, 1983) Applegate et al. in Covington & Wise, 1987
Prediscosphaera columnata	(Stover, 1966; Perch-Nielsen, 1984)
Prediscosphaera spinosa	(Bramlette & Martini, 1964) Gartner, 1968
Radiolithus hollandicus	Varol, 1992
Radiolithus planus	Stover, 1966
Repagulum parvidentatum	(Deflandre & Fert, 1954) Forchheimer, 1972
Retecapsa angustiforata	Black, 1971
Rhagodiscus achlyostaurion	(Hill, 1976) Doeven, 1983
Rhagodiscus angustus	(Stradner, 1963) Reinhardt, 1971
Rhagodiscus asper	(Stradner, 1963) Reinhardt, 1967
Rhagodiscus gallagheri	Rutledge & Bown, 1996
Rhagodiscus splendens	(Deflandre, 1953) Verbeek, 1977
Rotelapillus crenulatus	(Stover, 1966) Perch-Nielsen, 1984
Seribiscutum primitivum	(Thierstein, 1974) Filewicz et al. in Wind & Wise 1983
Sollasites falklandensis	Filewicz et al. in Wise & Wind, 1977
Sollasites horticus	(Stradner et al. in Stradner & Adamiker, 1966) Cepek & Hay, 1969
Staurolithites angustus	(Stover, 1966) Crux, 1991)
Staurolithites crux	(Deflandre & Fert) Caratini 1963
Staurolithites gausorhethium	(Hill, 1976;) Varol & Girgis, 1994
Staurolithites laffittei	Caratini, 1963
Staurolithites mutterlosei	Crux, 1989
Stoverius achylosus	(Stover, 1966) Perch-Nielsen, 1986
Stoverius protosignum	(Worsley, 1971) Young & Bown 2014
Tegumentum stradneri	Thierstein in Roth & Thierstein, 1972
Tetrapodorhabdus coptensis	Black, 1971
Tetrapodorhabdus decorus	(Deflandre in Deflandre & Fert, 1954) Wind & Wise 1983
Tranolithus orionatus	(Reinhardt, 1966a) Reinhardt, 1966b
Tubodiscus burnettiae	Bown in Kennedy et al., 2000
Watznaueria barnesiae	(Black in Black & Barnes, 1959) Perch-Nielsen, 1968
Watznaueria bayacki	Worsley, 1971
Watznaueria biporta	Bukry, 1969
Watznaueria britannica	(Stradner, 1963) Reinhardt, 1964
Watznaueria fossacincta	(Black, 1971) Bown in Bown & Cooper, 1989
Zeugrhabdotus (<4um)	
Zeugrhabdotus acanthus	Reinhardt, 1965
Zeugrhabdotus embergeri	(Noël, 1959) Perch-Nielsen, 1984
Zeugrhabdotus howei	Bown in Kennedy et al., 2000
Zeugrhabdotus scutula	(Bergen, 1994) Rutledge & Bown, 1996
Zeugrhabdotus trivectis	Bergen, 1994
Zeugrhabdotus xenotus	(Stover, 1966) Burnett in Gale et al., 1996